GE Nuclear Energy

TECHNICAL MODIFICATIONS SERVICES
GE-NE-523-B13-01869-043, Rev. 1

April 1997

ASSESSMENT OF THE VERTICAL WELD CRACKING ON THE NMP1 SHROUD

Prepared for

Niagara Mohawk Power Company

Prepared by

GE Nuclear Energy
175 Curtner Avenue
San Jose, CA 95125

ASSESSMENT OF THE VERTICAL WELD CRACKING ON THE NMP1 SHROUD

April 1997

Prepared by: S. Ranganath, Engineering Fellow

Prepared by: H. S. Mehta, Principal Engineer

Prepared by: for H. Choe, Principal Engineer

Prepared by: R. Horn, Engineering Fellow

Prepared by: B.A. McAllister, Manager
Reactor Internals Management

Reviewed by: T. A. Caine, Project Manager
Engineering and Licensing Consulting Services

Approved by: G. L. Hayes, Manager
Engineering and Licensing Consulting Services
Nuclear Services Department

EXECUTIVE SUMMARY

During the current refueling outage (RFO 14) at the Nine Mile Point Unit 1 (NMP1) Station, cracking was detected in the vicinity of vertical welds of the core shroud. The cracking was detected by inspections performed in accordance with industry recommendations. This report describes the evaluations of the vertical weld cracking. Based on evaluations which considered bounding crack growth rates and conservative crack sizing assumptions continued operation is justified for 10,600 hours (approximately 16 months).

Following the initial finding of the vertical weld indications, extensive inspections using automated ultrasonic (UT) and enhanced visual (EVT) examination techniques were performed to fully characterize each shroud vertical weld. Additional automated examinations were also performed on selected shroud horizontal welds however, since the shroud is supported by a tie rod repair which was installed in RFO 13 based on the assumption of throughwall cracking of horizontal welds (H-1 through H-7) as the design basis, no additional evaluation of horizontal weld inspection results is required.

A detailed evaluation was performed to determine the structural significance of the indications found in the vertical welds. Several conservative assumptions were made in the analysis:

- No credit was taken for any portion of horizontal welds; it is assumed that each section of the shroud is a free standing cylinder. Thus, the presence of horizontal weld cracking has no impact on the vertical weld crack assessment,

- A bounding crack growth rate of 5×10^{-5} inches per hour has been assumed. Field data and predictive models show that this is bounding even with irradiation effects. Furthermore, because of the excellent water chemistry at NMP1 (reactor water conductivity <0.1 μS/cm) the actual crack growth rates are expected to be much lower,

- All uninspected regions are postulated to be cracked throughwall,

- Allowance is made for crack sizing uncertainty in detected flaws.

The results of the fracture mechanics analyses summarized in the table below show that continued operation can be justified for 10,600 hours (approximately 16 months).

The results of the thermal hydraulic evaluation showed that even with postulated through wall cracking of the vertical welds, the resulting leakage has no safety impact. Furthermore, since the vertical weld cracks are within the allowable sizes, they have no impact on the effectiveness of the shroud repair which structurally replaces the horizontal welds.

Based on the evaluation presented, continued operation can be justified for 10,600 hours (approximately 16 months) and all of the required safety margins will be maintained.

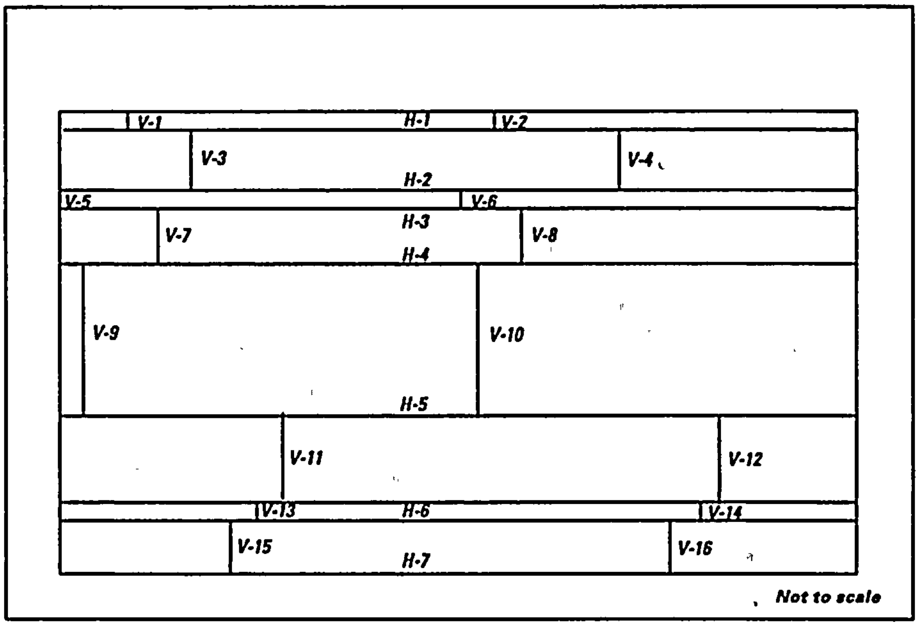

NMP1 Core Shroud Welds

Weld ID	Evaluation Period
V-3	16,000 hours (> 24 months)
V-4	10,600 hours (~ 16 months)
V-7, V-8	16,000 hours (> 24 months)
V-9, V-10	10,600 hours (~ 16 months)
V-11, V-12	16,000 hours (>24 months)
V-15, V-16	16,000 hours (>24 months)

TABLE OF CONTENTS

1. BACKGROUND	1
2. SUMMARY OF INSPECTION FINDINGS	4
3. PROBABLE CAUSE OF CRACKING	8
4. CRACK GROWTH ASSESSMENT	11
5. STRUCTURAL MARGIN ASSESSMENT	13
6. THERMAL HYDRAULICS ASSESSMENT	33
7. OVERALL SAFETY CONCLUSION	37
8. REFERENCES	38
APPENDIX A EFFECT OF TIE RODS ON VERTICAL WELD STRESS	A-1
APPENDIX B CRACK GROWTH RATE BASED ON THE GE THEORETICAL MODEL	B-1
APPENDIX C SHROUD INSPECTION SUMMARY	C-1

1.0 BACKGROUND

During the current refueling outage (RFO 14) at the Nine Mile Point Unit 1 (NMP1) Station cracking was detected in the vicinity of vertical welds of the core shroud. Figures 1-1 and 1-2 show a detailed view of certain shroud weld locations. This cracking was detected by inspections performed in accordance with industry recommendations as described in the BWRVIP Guidelines for Reinspection of Core Shrouds (Reference 1).

In March of 1995 (RFO 13), a GE designed tie rod repair was installed on the shroud. The purpose of the tie rod repair was to provide adequate support to allow the shroud to perform its function under normal operation and accident conditions with postulated through wall cracking at horizontal welds (H-1 through H-7). The tie rod repair has been demonstrated to have no impact on the cracking that has been detected on shroud vertical welds (See Section 3.1).

During RFO 13, consistent with recommendations for the installation of the repair, visual inspections were performed on limited areas of the shroud vertical welds in the core region from the inside of the shroud. No cracking was detected.

Since the inspections performed in RFO 13, the BWRVIP has issued guidelines for reinspection of the shroud (Reference 1). The recent inspection was performed according to these guidelines, and unlike the previous vertical weld inspection in RFO 13, it focused on a sample inspection from the outside diameter (OD) of the shroud. Cracking was initially detected at the V-10 weld. The inspection scope was then expanded to include accessible areas of all vertical welds. This inspection scope expansion detected cracking at other shroud vertical weld locations.

The purpose of this report is to assess the safety consequences of cracking detected at vertical shroud welds on the operation of the NMP1 Station.

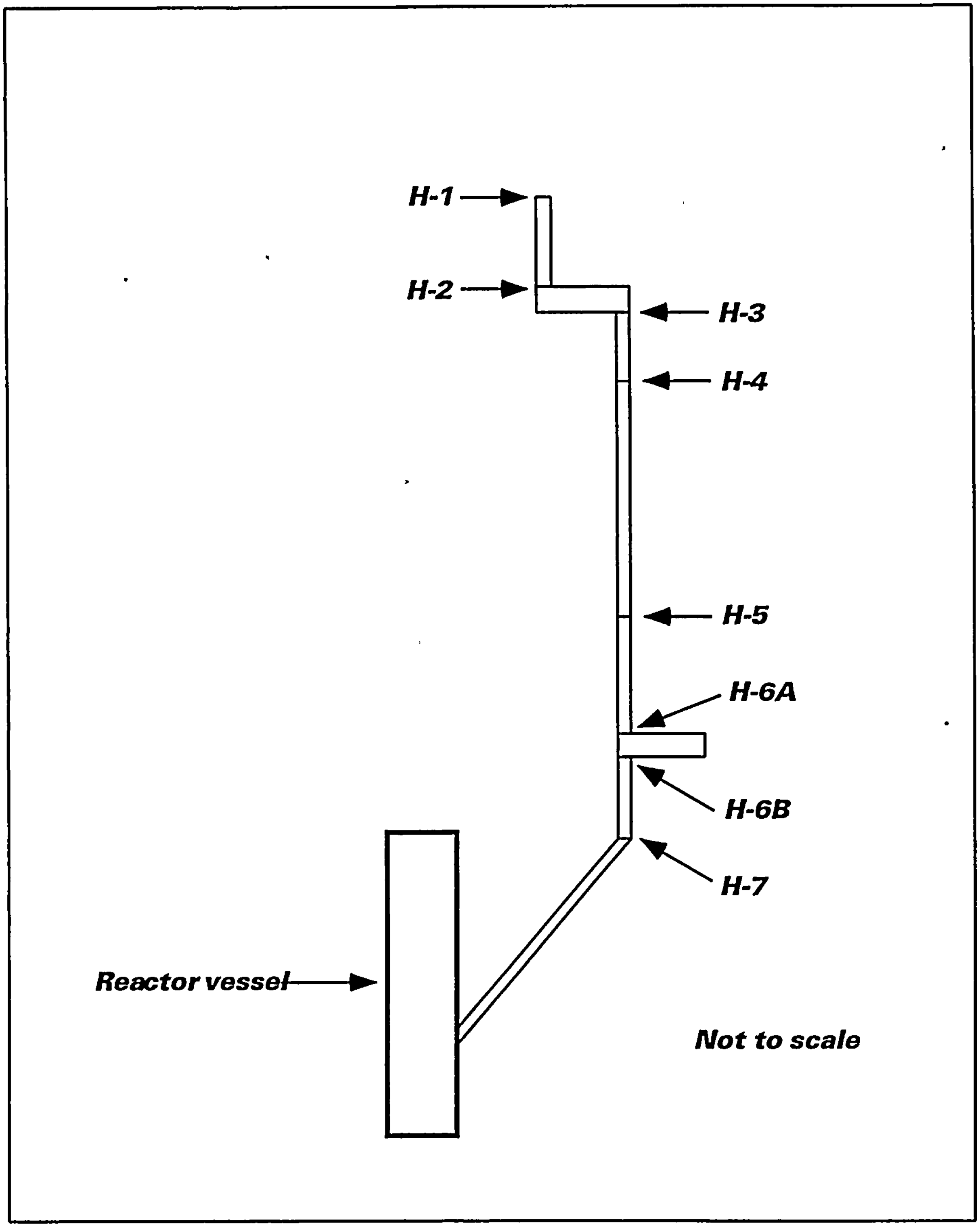

Figure 1-1 NMP1 Shroud Weld Locations, Cross Sectional View

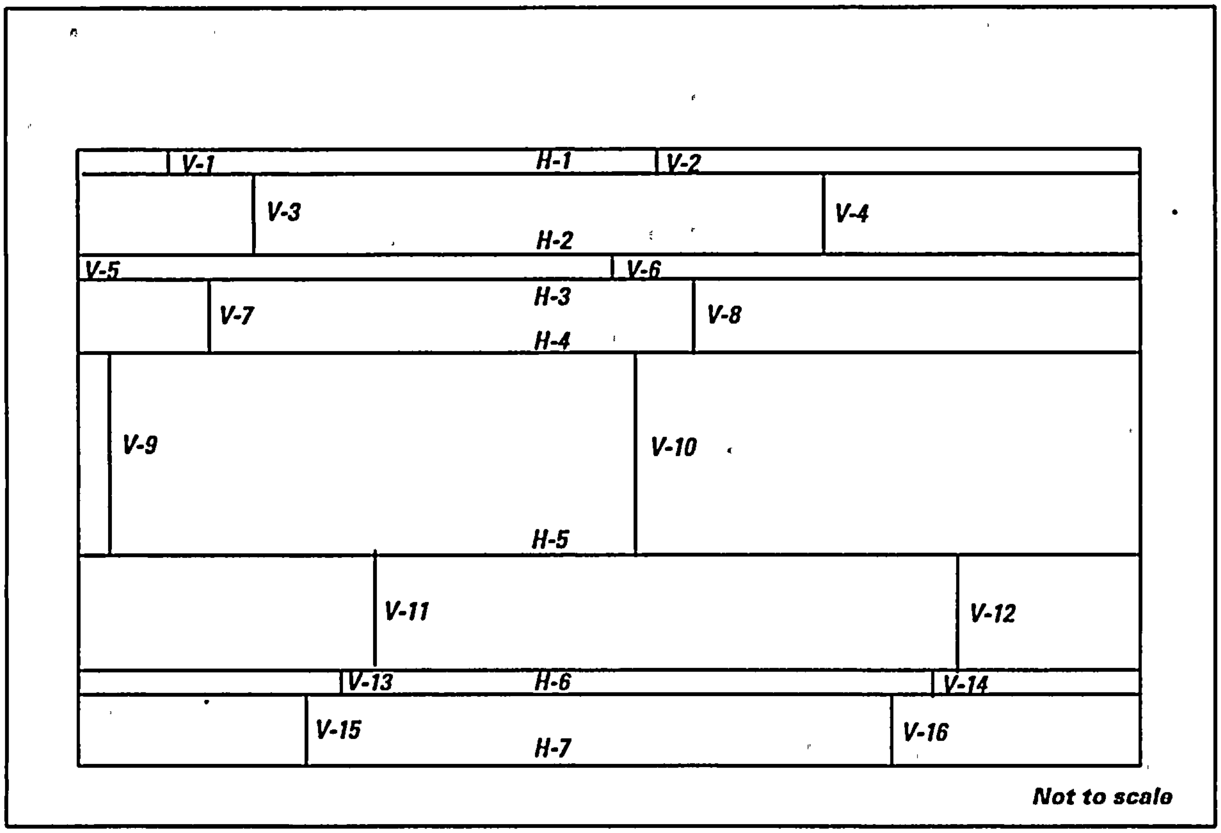

Figure 1-2 NMP1 Shroud Weld Locations

2.0 SUMMARY OF INSPECTION FINDINGS

2.1 Previous Inspections

During RFO 13 limited inspection of shroud vertical welds V-9, V-10, V-11, and V-12 was performed by enhanced visual examination techniques. The exam was performed on the inside diameter of the shroud and the coverage included a six inch portion of the welds at the location of the intersection of horizontal weld H-5. At that time the inspection scope was considered adequate because of the limited reported incidences of vertical weld cracking and the large flaw tolerance of vertical welds. During that examination, no cracking was detected on welds V-9, V-10, and V-11. Weld V-12 was not located. In addition, examination of ring segment welds V-5 and V-6 was attempted, however these welds were not located. These results are summarized in Table 2-1. It should be noted that these regions examined during RFO 13 showed no indications during the recent inspections conducted during RFO 14.

2.2 Recent Inspection Results for Shroud Vertical Welds

The recent inspections were performed in accordance with BWRVIP guidelines for reinspection of the shroud (Reference 1). These guidelines require visual inspection from the outside diameter (OD) surface or inside diameter (ID) surface, of 25% of the equivalent length of all vertical welds.

The planned inspection scope included portions of vertical welds V-9 or V-10, and V-11, and either ring segment welds V-5 or V-6, (contingent upon locating these welds) from the outside diameter. Cracking was initially detected at the V-10 weld.

The inspection scope was then expanded as required by the BWRVIP guidelines to include accessible areas of each vertical weld. Extensive examinations were then performed to fully characterize the shroud vertical weld cracks on both the inside diameter and outside diameter of the shroud. Both ultrasonic (UT) and enhanced visual examination (EVT) techniques were used to achieve maximum characterization of the vertical weld regions. These examinations were performed in accordance with BWRVIP Examination Guidelines (Reference 2).

The current inspections revealed fairly significant cracking on welds V-4, V-9, V-10, relatively minor cracking on welds V-3, V-12, V-15, and V-16, and no cracking on the accessible regions of welds V-7, V-8, and V-11. A summary of these examinations are provided in Table 2-2. A detailed description of the scope and findings are provided in Appendix C.

Examinations were performed in an attempt to locate ring segment welds V-5 and V-6 using eddy current and visual inspection techniques. The inspections to date of the accessible areas of the ring could not locate the vertical welds, but found no cracking either.

Additional examinations were also performed on selected horizontal welds however, since the shroud is supported by the tie rod repair which assumes through wall cracking of horizontal welds (H-1 through H-7) as the design basis, no additional evaluation of horizontal weld inspection results is required. A summary of the horizontal weld inspections is also provided in Appendix C.

Table 2-1
Summary of Previous Shroud Vertical Weld Inspections (RFO 13)

Weld	Inspection Coverage	ID or OD of shroud	Exam Type	Results
V-9	6 " from H-5	ID	Enhanced visual, EVT-1 (Ref. 2)	No Indications
V-10	6 " from H-5	ID	EVT-1	No Indications
V-11	6 " from H-5	ID	EVT-1	No Indications
V-12	6 " from H-5	ID	EVT-1	Weld not located

Table 2-2
Summary of Recent Shroud Vertical Weld Inspections (RFO 14)

Weld	Weld Length (in)	Inspection Coverage*	Shroud ID/OD	Exam Type	Flaw Length
V-3	31.25	15" Left 15" Right	OD	UT	1.5" ID, Right HAZ 0.8" OD, Right HAZ
V-4	31.25	22" Left 11" Right	OD	UT	22"ID Left HAZ, 1.5"ID Right HAZ
V-5 ring		Not located	NA	NA	NA
V-6 ring		Not located	NA	NA	NA
V-7	18.5	9" Left 11" Right	OD	UT	No Indications
V-8	18.5	5.5" Left 9.5" Right	OD	UT	No Indications
V-9 shell	90.12	100%	ID and OD	EVT-1	Indications on over 90% OD right HAZ Minor cracking on OD left side and on ID both sides
		80"	OD	UT	Numerous indications on OD, Left HAZ Two minor flaws on ID, Right HAZ
V-10	90.12	100%	ID and OD	EVT-1	Cracking on OD, Right HAZ Cracking on ID, Left and Right HAZ
		84"	OD	UT	Flaws detected on > 80% on OD, Right HAZ Flaws detected on > 10% on OD, Left HAZ
V-11	63.5	100% OD 50% ID	ID and OD	EVT-1	No Indications
V-12	63.5	100% OD 50% ID	ID and OD	EVT-1	6" OD, Right HAZ
V-15	22.13	11" Left 11" Right	OD	UT	6" ID, Left HAZ 2.2" ID, Right HAZ
V-16	22.13	100%	OD	EVT-1	.75" OD, Left HAZ
		10.5" Left 20" Right	OD	UT	5" ID Left HAZ 4" ID Right HAZ 3" ID Left HAZ from right side exam

* The inspected regions indicated on each side of the weld are not necessarily coincident, hence the integrated inspection coverage may be less than indicated, but has been taken into account in determining the uncracked ligament length.

3.0 PROBABLE CAUSE OF CRACKING

It is believed that the cause of shroud vertical weld cracking is Intergranular Stress Corrosion Cracking (IGSCC). The stresses that cause cracking in vertical welds are weld residual and fabrication stresses and to a lesser extent the stress resulting from internal pressure, which is hoop stress. Although the tie rod repair is not expected to add any additional hoop stress to the vertical welds, a detailed analysis was performed to demonstrate this. The results of this evaluation are summarized below. A discussion of the overall SCC susceptibility of vertical shroud welds is also provided.

3.1 Effect of Tie Rod Loads

A three dimensional finite element analysis was performed to demonstrate that the thermal preload associated with the tie rod shroud modification has a negligible impact on the potential for crack growth in the shroud vertical welds. The NMP1 shroud modification consists of four sets of tie rod assemblies that are mechanically and thermally preloaded with sufficient force to prevent separation of the shroud sections at the locations of horizontal welds under normal operating pressures. This tie rod preload introduces a vertical compressive stress. The stresses that can cause vertical weld cracking are the weld residual stress and to a lesser extent the stress resulting from internal pressure, which is hoop stress. The three dimensional finite element analysis showed that any hoop stress induced at the vertical welds due to tie rod compression is negligible. The details of this analysis are provided in Appendix A. Based on this analysis it is concluded that the shroud tie rod modification did not cause shroud vertical weld cracking.

3.2 Susceptibility to Intergranular Stress Corrosion Cracking (IGSCC)

It has been recognized that all BWRs could be affected to some extent by IGSCC of the core shroud. The critical factors that can affect cracking are the following: operating time, coolant conductivity, material carbon content, orientation (short transverse plate orientation exposed to coolant), fabrication related surface cold work, neutron fluence, and stresses due to welding and fabrication as well as operating stresses. These factors that affect IGSCC apply to both the horizontal and vertical welds in the shroud. They also have been used as a guide for establishing the timing of shroud weld inspections

which have been performed over the last four years at a number of operating BWRs. The focal point for inspections has been the shroud horizontal welds based on the initial observations of cracking.

The experience in BWRs has shown that IGSCC initiation and growth is related to operating time. The initiation process is a stochastic process and with time the probability of cracking increases. This process can be accelerated if the water conductivity is higher because impurities aid crack initiation and accelerate crack growth. The characteristics of the coolant environment are also known to promote IGSCC on both the outside and the inside of the shroud. Although NMP1 has experienced long operating times and relatively higher reactor conductivity values in the early operating years, recent operation has been with excellent water chemistry as shown by the low values of reactor water conductivity in the past operating cycle ($< 0.1\ \mu S/cm$).

The material susceptibility can be influenced by several factors. The likelihood of sensitization occurring in the heat affected zone (HAZ) during the welding process is directly related to the carbon level of the stainless steel materials used. Type 304 stainless steel material with greater than 0.04% carbon was consistently used in the earlier plants. The carbon content in the Type 304 SS materials used to fabricate the NMP1 shroud ranged from 0.042 to 0.062%.

The susceptibility of the material is also related to the amount of surface cold work present. For NMP1, portions of the shroud were subjected to cold working. By itself, the cumulative cold work from the different stages of fabrication can have a marked effect on crack initiation. Cold working can also introduce martensite, which will synergistically harden the surface and will sensitize over time at the operating temperatures.

Another factor that contributes to IGSCC is stress. The welding process introduced high residual stresses in the shroud welds. These residual stresses have been shown to vary in magnitude over the length of the welds, and are often found to reach the yield strength of the plate material. Fabrication can also introduce fit-up stresses. The largest fit-up stress would be expected in the last step of the assembly with the manufacture of the H-4 weld which has exhibited some cracking.

The final factor is that of irradiation. Irradiation can affect the material's susceptibility throughout the thickness, with expected slightly larger effects on the inside surface. The

material's susceptibility is expected to increase from the material's initial sensitization thereby further promoting IGSCC in the locations of highest residual stress and cold work. However, irradiation also reduces the weld residual stresses, which has the effect of slowing crack growth rates.

In summary, the Nine Mile Point Unit 1 shroud horizontal and vertical welds are clearly susceptible to IGSCC. The high carbon Type 304 stainless steel material was initially sensitized by the welding process. The material's susceptibility was further enhanced by surface cold work and surface strains from the fabrication processes. Irradiation would also add to the susceptibility over the operating time. Finally, the tensile surface residual stresses and surface fabrication stresses led to IGSCC initiation.

4.0 CRACK GROWTH RATE ASSESSMENT

The crack growth rate in the vertical welds for the next cycle of operation was predicted using several methods. The following four methods were used: (1) the NRC accepted K-Dependent curve, (2) the BWRVIP correlation (Reference 3), (3) the PLEDGE correlation, and (4) the SKI crack growth model (Reference 4). The calculations were performed for a range of stress intensities. For the BWRVIP and PLEDGE correlations, a reactor water conductivity equal to 0.1 μS/cm, an ECP of 200 mV (SHE), and an initial sensitization (EPR) equal to 15 C/cm^2 were used. The results of these calculations are provided in Table 4-1.

The NRC bounding crack growth rate is characteristic of higher reactor water conductivity environments (~0.3 μS/cm). Improvement in the reactor water conductivity can reduce the crack growth rate significantly. The reactor water conductivity at NMP1 for the year 1996 was on the average 0.09 μS/cm. This value indicates that at present the water chemistry is excellent and is one of the best in the BWR fleet. Assuming that this conductivity is maintained for the next cycle, the predicted average crack growth rate is expected to range from 1×10^{-5} in/hr to 2.3×10^{-5} in/hr (for an average stress intensity across the thickness of the plate equal to 20 ksi$\sqrt{in}$). These rates are much less than the NRC bounding rate of 5×10^{-5} in/hr.

Irradiation can affect crack growth rates and was not explicitly considered in the crack growth predictions except for the BWRVIP correlation which was benchmarked by the crack growth data measured on shroud welds for various range of fluence.

An evaluation was performed that compares the GE PLEDGE model predictions for unirradiated material to the predictions for irradiated materials at these same values of reactor water conductivity, ECP, and initial sensitization. This comparison shows that at fluence levels expected for BWR shrouds the predicted crack growth rate is comparable for both the unirradiated and the irradiated models. The similarity in rates can be attributed to offsetting effects. While the irradiation increases the susceptibility of the material (EPR increases), it also causes relaxation of the weld residual stresses reducing the driving force for crack growth. Because the radiolysis effects are included through ECP, the unirradiated PLEDGE model can be used to predict the crack growth rate for these conditions. For completeness, the details of the irradiation evaluation are provided

in Appendix B. This evaluation (Refer to Figure B-12) also shows that for the expected reactor water conductivity, ECP, and EPR accounting for irradiation, the crack growth rate over the range of shroud fluences is bounded by the NRC bounding crack growth rate of 5 x 10^{-5} in/hr. Consistent with the different models, the crack growth rate is expected to be less than this value based on field data from operating plants.

Finally, UT data obtained during the current outage (RFO 14) for the H-8 crack that was detected and measured in the 1995 outage (RFO 13) has shown that the crack has not grown. This provides additional data to support that the crack growth rate is expected to be much lower than the NRC bounding rate.

Table 4-1
Predicted Crack Growth for Different Models

Model	NRC K-Dependent Curve (Upper Curve)	BWRVIP Correlation*	PLEDGE*	SKI Crack Growth Model*
Stress Intensity = 10 ksi-in$^{1/2}$	5 x10^{-6} in/hr	1.6 x 10^{-6} in/hr	4.2 x 10^{-6} in/hr	1.7 x 10^{-6} in/hr
Stress Intensity = 15 ksi-in$^{1/2}$	1.2 x 10^{-5} in/hr	3.8 x 10^{-6} in/hr	1.1 x 10^{-5} in/hr	5.7 x 10^{-6} in/hr
Stress Intensity = 20 ksi-in$^{1/2}$	2.3 x10^{-5} in/hr	7.1 x 10^{-6} in/hr	2.3 x 10^{-5} in/hr	1 x 10^{-5} in/hr
Stress Intensity = 25 ksi-in$^{1/2}$	3.7 x 10^{-5} in/hr	1.1 x 10^{-5} in/hr	4.0 x 10^{-5} in/hr	1.9 x 10^{-5} in/hr

Bounding Crack Growth Rate Used by the Industry = 5 x 10^{-5} in/hr

***Conductivity = 0.10 μS/cm; ECP = 200 mV, SHE; Initial Sensitization = 15 C/cm^2**

5.0 STRUCTURAL MARGIN ASSESSMENT

The shroud repair that was implemented for assumed throughwall cracking of shroud horizontal welds does not require the vertical welds to be crack free. The repair allows the presence of vertical weld cracks, as long as the crack lengths are less than the allowable flaw sizes or as long as the structural integrity of the vertical weld can be demonstrated. Therefore, assuming that the vertical flaw sizes are smaller than the allowables or that structural integrity can be demonstrated, the validity of the tie rod repair modification is maintained.

The primary stress which could cause vertical weld failure results from the internal pressure. Consistent with ASME Code practice (Appendix C, Section XI), internal pressure is the only load to be considered for axial cracks. Other loads such as seismic have negligible impact and need not be considered. The value of the internal pressure varies from plant to plant, but is typically small (less than 15 psi above the core plate for normal operation). The allowable flaw sizes consider the internal pressures under all conditions - normal, upset, and accident events, with the appropriate safety factors. Typically, the allowable crack sizes are large and approach and/or exceed the length of the weld itself, indicating large crack tolerance.

No credit is taken for the horizontal weld integrity in determining the allowable vertical weld flaw sizes. The horizontal welds are assumed completely cracked through-wall, 360°, and the cylinder between any two horizontal welds is assumed to be 'stand-alone'. The calculations also assume simultaneous cracks at the diametrically opposite welds in a given cylinder. Furthermore, the cracking is assumed to be through wall. Both LEFM and limit load are considered in developing the allowable flaw sizes. The actual allowable flaw size is the lower of the allowables for each of the two methods. The required minimum ligament calculations also include allowances for crack growth and inspection uncertainty.

Multiple cracking of vertical welds is not a significant concern since the analysis assumes that the upper and lower horizontal welds are completely cracked, and treats each cylinder independently. Multiple cracks in a single weld also do not pose any concern since the fracture analysis includes proximity effects and also crack growth to account for possible linking of two separate cracks. The shroud repair includes the consideration of multiple fully cracked horizontal welds. Therefore, as long as the allowable vertical flaw size within

each cylinder is not exceeded or the structural integrity of each vertical weld within each cylinder can be demonstrated, the presence of multiple vertical weld cracking is not a concern.

This section first presents the details of a screening criteria analysis which gives the required value of the uncracked ligament length (difference between the length of weld and the allowable flaw size) at each of the vertical welds in the shroud, assuming that regions with indications are cracked throughwall. If this criteria length is not satisfied at a shroud vertical weld, a more detailed fracture mechanics analysis is necessary to demonstrate the integrity of a vertical weld with indications.

5.1 Required Uncracked Ligament Lengths by Screening Criteria

For this calculation it is conservatively assumed that the different sections of the shroud are in fact free standing cylinders (i.e., fully cracked circumferential welds). With this assumption, it is possible to determine the required uncracked weld length at each of the vertical welds in the shroud. Allowable vertical weld flaw sizes are based upon a set of reactor internal pressure differences. Table 5-1 documents the pressure differentials used in the calculation (Reference 5).

Allowable shroud vertical crack lengths were calculated based on both linear elastic fracture mechanics (LEFM) and limit load analysis. The high fluence region where there is potential irradiation embrittlement is limited to the shroud section between horizontal welds H-3 and H-6a. Therefore, both LEFM and limit load analysis were used for vertical welds in this region. Specifically, LEFM was governing for the welds V-9, V-10, V-11, and V-12 and limit load was governing for welds V-7, and V-8. The vertical welds in other regions were governed by limit load analysis. Both methods of analysis are described below.

5.1.1 Linear Elastic Fracture Mechanics (LEFM)

The stress intensity factor for a through thickness axial crack of length 2a, in an infinite cylinder is given by:

$$K = M\sigma_m\sqrt{\pi a}\ , \qquad [1]$$

where σ_m is the nominal hoop stress, and M is a factor that accounts for curvature effects, and is given by (Reference 5):

$$M = (1.0 + 1.25\lambda^2)^{0.5} \qquad \text{for } 0.0 \le \lambda \le 1.0 \qquad [2a]$$
$$= 0.6 + 0.9\lambda \qquad \text{for } 1.0 \le \lambda \le 5.0 \qquad [2b]$$
$$\lambda = a/\sqrt{(Rt)} \qquad [2c]$$

where 'a' is the half crack length, as defined above; 'R' is the mean radius of the shroud; and 't' is the shroud thickness.

Equation 1 assumes a cylindrical shell of infinite length (Figure 5-1a). This is a reasonable assumption for the realistic cases where limited cracking (part through cracking) is observed. With this assumption, in most cases the allowable through wall crack length exceeds the length of the weld seam itself, confirming the large crack tolerance for vertical welds. However, the design postulated for the shroud repair assumes that each circumferential weld has 360° through thickness cracking. This essentially means that each shell course between two horizontal welds should be considered as a separate, free standing finite width cylindrical shell (similar to a drum open at both sides). In order to account for the finite width of the shroud section being considered, a finite width correction factor given by $\sqrt{\sec}\,(\pi a/2b)$ is applied (Figure 5-1b). This is based on correction factors for through thickness cracks in plates (Reference 6), and when used in conjunction with the curvature correction factor for the shell provides a reasonable representation for a through thickness crack in a finite width cylindrical shell.

The final form of K used for this analysis becomes:

$$K = \sigma_m\sqrt{\pi a}\cdot M\cdot\sqrt{\sec\frac{\pi a}{2b}}\ , \qquad [3]$$

where 2b is the height of the shroud section being considered.

The calculated stress intensity factor when multiplied by the appropriate safety factor (3 for normal/upset conditions and 1.5 for emergency/faulted conditions) can be compared with the available fracture toughness of 150 ksi√in and the allowable through wall crack length (with the required safety factor) can be determined. For example, for vertical welds V-9 and V-10, the allowable through wall crack length was determined to be 75.4 inches (or a = 37.7 in.). For this case, the value of factor λ per Equation (2c) is [37.7/√(179*1.5/2)] or 3.25. The factor M per Equation (2b) is then 3.52.

The value of K is then calculated as shown below:

$$K = 1.969 ksi \sqrt{\pi \cdot 37.7 in} \cdot 3.52 \cdot \sqrt{\sec \frac{\pi \cdot 37.7 in}{90.12 in}} = 149.7 ksi \cdot \sqrt{in} . \qquad [4]$$

The stress 1.969 ksi corresponds to the calculated hoop stress for 22 psi (faulted condition) including the safety factor of 1.5. This means that an allowable flaw size of 75.4 inches is acceptable. As expected, because of the finite width cylinder assumption, the allowable crack length is less than the width of the shell course for V-9 and V-10, in this case 90.12 inches for Nine Mile Point Unit 1. Alternatively, the required uncracked ligament is 90.12 - 75.4 = 14.72 inches. The required ligament is increased when the effects of NDE uncertainty and crack growth are included.

5.1.2 Limit Load Analysis

The limit load analysis applies to all welds and the allowable crack size is the smaller of the limit load and LEFM (where applicable) crack lengths. The limit load calculations were performed using concepts similar to those described in Section XI, Appendix C of the ASME Code. For the limit load analysis, the minimum required ligament is calculated as the uncracked section of the weld needed to resist a force due to the pressure differential across the shroud (Figure 5-2). This pressure P, acts upon a

projected area D*L on the shroud, where D is the inside diameter of the shell segment, and L is the height of the shell course. Therefore,

$$P \cdot D \cdot L = 2 \cdot \left(\frac{\sigma_f}{SF} \cdot \ell \cdot t \right) , \qquad [5]$$

where σ_f is the flow stress (assumed to be equal to $3S_m$ where S_m is the ASME Code allowable design stress intensity, equal to 16.9 ksi for the shroud material at 550°F), SF is the safety factor, ℓ is the required uncracked ligament length, and t is the thickness of the shroud. This assumes that the entire weld except for the ligament has through thickness cracking. It also considers, conservatively, cracking on both sides as shown in Figure 5-2.

Rearranging Equation 5 and noting the definition of hoop stress, the following results:

$$SF \cdot \frac{P \cdot D}{2t} \cdot \frac{L}{\sigma_f} = \ell \qquad [6]$$

$$SF \cdot \sigma_m \cdot \frac{L}{\sigma_f} = \ell \qquad [7]$$

where σ_m is once again the nominal hoop stress for this shell segment. In determining the required uncracked ligament, the bounding case of normal/upset conditions (SF = 3.0) and faulted conditions (SF = 1.5) should be considered. As stated earlier, the analysis for the required ligament is conservative since cracking is assumed on both sides.

5.1.3 Required Uncracked Ligaments

Table 5-2 shows the allowable crack length as well as the required uncracked ligament lengths for each vertical weld. Welds V-7 through V-12 were evaluated using both LEFM and limit load methods. LEFM was controlling for welds V-9 through V-12, and limit load was governing for all other welds. The recent BWRVIP criteria for reinspection of shrouds (Reference 1) recommends that allowances for crack growth (based on an assumed crack growth rate of 5 x 10^{-5} in/hr) and uncertainty in the inspection be added to the required uncracked ligaments. Assuming 8000 hot operating hours per year and a

two year cycle, the adder for growth in the crack length is (5 x 10^5 in/hr x 8000 hr/year x 2 years) x 2 =1.6 inch where the factor of two accounts for crack growth at two crack tips. The BWRVIP criteria also recommends adding an inspection uncertainty factor to each end of the observed indication length based on BWRVIP-03 (Reference 2). The uncertainty factor is (0.372")x 2 or 0.75 inch for ultrasonic examination (UT). Essentially, this means that the required uncracked ligament length be increased by (0.75 + 1.6) or 2.35 inch to account for the crack growth and UT inspection uncertainty. Similarly, for enhanced visual examination, the uncertainty factor is (1.2") x 2 or 2.4 inch, thus the required uncracked ligament length be increased by (2.4 + 1.6) or 4.0 inch to account for the crack growth and EVT inspection uncertainty

Table 5-2 Column 5 lists the calculated values of required ligament lengths for various vertical welds. A comparison of these values with the values determined by the examinations of these welds is discussed next.

Cracking of radial ring welds was separately evaluated and found to have negligible impact. The only effect of radial ring weld cracking is on the thermal preload but it was found that even with 90% of the weld assumed to be cracked, the effect on preload was insignificant. Therefore ring weld cracking is not significant from a structural viewpoint and no inspection is required. Nevertheless, attempts were made to inspect the V-5 and V-6 ring welds using eddy current and visual techniques. The inspection of the accessible areas of the entire ring could not locate the welds but found no cracking either.

5.2 Comparison with Required Uncracked Ligament Lengths

Column six in Table 5-2 lists the values of uncracked ligament lengths determined from the UT and EVT examination of the various shroud vertical welds. A comparison of these lengths with those required by the conservative screening criteria lengths (Column 5) shows that each of the vertical welds except V-4, V-9 and V-10 meets the required uncracked ligament length criteria. A detailed evaluation for welds V-4, V-9 and V-10 is described in the next subsection.

5.3 Evaluation of Welds V-9, V-10, and V-4

The previous section described the evaluation of the vertical welds assuming the following:

1. Cracks were assumed to be through wall in uninspected regions.

2. Both LEFM and limit load failure mechanisms were considered, and the allowable flaw sizes were determined using the ASME Code specified safety factors.

3. A bounding crack growth rate of 5×10^{-5} inches per hour was used in all crack growth analyses. Appropriate uncertainty factors were used on the crack sizing.

4. Where indications were found either by UT or VT, they were assumed to be through wall.

5. Evaluation was performed for a period of 16,000 hot operating hours (2 years) and the indications were deemed acceptable if the final crack length after crack growth was within the allowable value.

Based on this conservative bounding evaluation, each weld except V-4, V-9 and V-10 was shown to be acceptable for continued operation for at least one fuel cycle (16,000 hours). This section describes the detailed evaluation of these three welds separately to determine the allowable period of operation. The first three assumptions were used in this assessment also, but credit for uncracked ligaments was included for part through cracks after accounting for crack growth. The allowable flaw size was determined with the appropriate safety factors and the allowable period of operation was determined. Of the three welds, V-9 and V-10 are more limiting and were therefore first evaluated.

5.3.1 Evaluation of the V-9 and V-10 Welds

Figures 5-3 and 5-4 show the UT determined depths for welds V-9 and V-10, respectively as a function of distance from weld H-4. Superimposing the depths of weld V-10 on V-9 (Figure 5-5), it is seen that weld V-9 is more limiting and is therefore selected for detailed assessment. Figure 5-6 shows the crack depth profile of V-9 after considering crack growth for 10,600 hours (approximately 16 months) and including a UT uncertainty factor of 0.1 inch on depth. The increment in depth is the crack growth ($10{,}600 \times 5 \times 10^{-5} = 0.53$ in.)

plus the UT allowance of 0.1 inch giving a total change of 0.63 inch. As discussed later, the choice of 10,600 hours was based on the fact that the stress intensity factor corresponding to the cumulative crack depth at 10,600 hours was equal to the allowable stress intensity factor of 150 ksi√in.

The projected crack depth after 10,600 hours shown in Fig 5-6 is based on bounding crack growth rates as well as conservative cracking assumptions (e.g. assuming all uninspected areas to have through wall cracking) and shows that a part of the crack becomes through wall and the remainder of the cracking is part through. The part through segment has a depth of 1.35 in. (or a ligament of 0.15 in.) while the main through wall segment has a conservatively estimated length of 32.5 inches. This crack is idealized as a compound crack as shown in Figure 5-7. The crack is acceptable if the required safety margins are demonstrated. Consistent with the ASME Code Section XI criteria for piping, the safety factor for normal and upset conditions is 3 and the corresponding value for faulted conditions (accident events such as steam line break) is 1.5. For the V-9 weld axial cracking the primary loading is the internal pressure - 8.9 psi for normal and upset conditions and 22 psi for the steam line break event. After applying the appropriate safety factors, it is seen that the accident condition is governing. For the analysis presented here a pressure of 22 x 1.5 = 33 psi is used. Since the safety factor is already included in the pressure, the results can be directly compared with the allowables, 150 ksi√in for the stress intensity factor and 3 S_m for the limit load analysis. The details of the fracture mechanics and limit load analysis are presented here.

LEFM Analysis

Since there were no standard handbook stress intensity factor solutions available for the compound crack shown in Figure 5-7, a detailed three dimensional finite element model (FEM) with special crack tip elements was developed to determine the stress intensity factors. Figure 5-8 shows the FEM and Figure 5-9 shows the details of the crack tip elements. The shroud segment was modeled with three dimensional brick elements and the crack region was modeled with crack tip elements which include the crack tip singularity and directly provide the stress intensity factors. A 180° segment was modeled and symmetry was assumed to represent the entire shroud. Sufficiently small mesh size (0.025 in.) was used in the crack region near the intersection of the part through and through wall crack segment. Comparison of the FEM results with and without the axial compression

due to the tie rod preload showed that the differences were negligible. Therefore, the subsequent analysis was based on having no axial load. The ends of the model near the H-4 and H-5 welds were free so that it simulated a free standing cylinder with no structural benefit from the integrity of the horizontal weld. As described before, an internal pressure of 33 psi was applied. The FEM analysis was qualified by comparing the results for simpler cases where handbook stress intensity factor solutions were available. For a through wall crack without the part through segment, comparison with closed form results showed good agreement confirming that the model was sufficiently refined. The analysis was performed with different crack depth (for the part through segment) cases and it was determined that for a crack depth of 1.35 inches, the FEM calculated stress intensity factor is approximately 150 ksi$\sqrt{in}$, which is the irradiated fracture toughness. This value is based on toughness measurements using specimens made from a plug sample taken from the shroud near the H-4 weld in an operating BWR. The fluence associated with the sample was 8 x 10^{20} n/cm ^{2}. This is higher than the estimated peak fluence for the NMP1 shroud, so the evaluation is conservative. The operating time corresponding to the 1.35 inch depth is 10,600 hours. Therefore, based on the conservative crack growth rates, and crack sizing, continued operation can be justified for 10,600 hours while maintaining the required Code fracture margins.

Limit Load Analysis

In addition to the fracture analysis, it is necessary to show that adequate limit load margins can be assured for the crack depth of 1.35 in. The results in Table 5-2 show that the required uncracked ligament for the V-9 weld is 3.51 in, or alternatively, the required area is 3.51 x 1.5 = 5.26 in^2. For the compound crack shown in Fig 5-7, the available area is approximately 7 in^2, which is in excess of the required value. Thus, the limit load criteria are met.

The evaluation shows that continued operation can be justified for 10,600 hours (approximately 16 months) while still meeting the required margins on fracture toughness as well as limit load.

5.3.2 Evaluation of the V-4 Weld

The crack depths for the V-4 weld are shown in Figure 5-10. The crack depth after crack growth for 10,600 hours and including the UT uncertainty allowance of 0.1 inch is also shown in the figure. Since the V-4 weld is above the top guide support ring, the fluence is sufficiently low so that the material is not embrittled and ductile behavior is assured. Therefore, fracture assessment is not needed and only limit load evaluation is necessary. Table 5-2 shows that the required uncracked ligament considering limit load is 1.28 inches, or alternatively, the required uncracked area after crack growth is 1.28 x 1.5 = 1.92 in^2. From the crack depth plot shown in Figure 5-10, the available area was calculated to be in excess of the required area for the V-4 weld. Therefore, the limit load margins are satisfied for the V-4 weld for a period of 10,600 hours.

5.4 Conclusions Concerning Structural Integrity

The structural analysis presented here shows that continued operation can be justified for at least 10,600 hours. In evaluating the structural safety, it is useful to identify the conservatisms used in the analyses:

- No credit was taken for the horizontal welds; it is assumed that each section of the shroud is a free standing cylinder. UT of the H-4 and H-5 welds has confirmed that there are significant uncracked areas so that it may be possible to show that even with through wall cracking of the V-9 and V-10 welds, structural integrity is maintained.

- A bounding crack growth rate of 5×10^{-5} inches per hour has been assumed. The crack growth discussion shows that even after considering potential IASCC contributions, the actual crack growth is expected to be lower than the bounding value used in the analysis.

- Allowance is made for crack sizing uncertainty for detected flaws,

- It is assumed that all uninspected regions are cracked through wall,

- The allowable hours of operation assures that the required ASME Code margins are maintained, considering both fracture and limit load mechanisms.

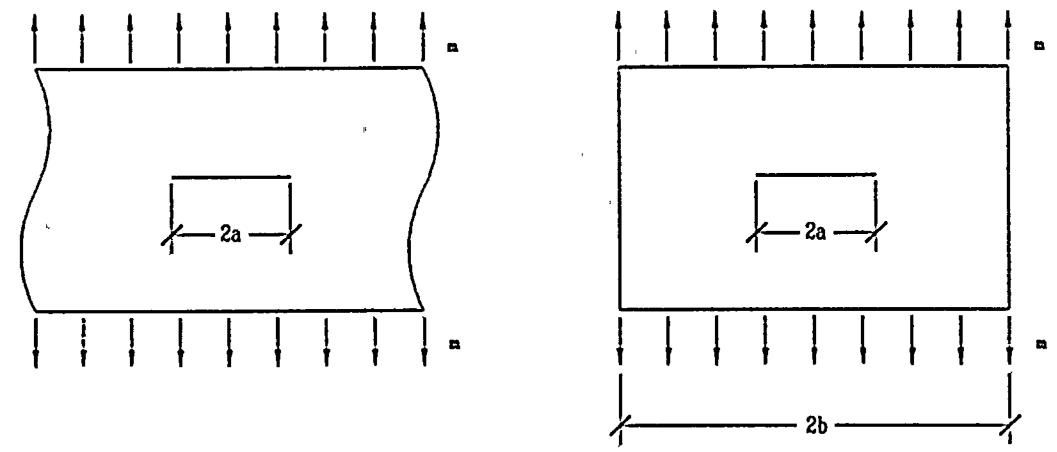

$$K = \sigma_m \sqrt{\pi a}$$

a) Infinite Plate

$$K = \sigma_m \sqrt{\pi a} \cdot \sqrt{\sec \frac{\pi a}{2b}}$$

b) Finite Plate

Figure 5-1 Infinite and Finite Width Plate With Through Cracking

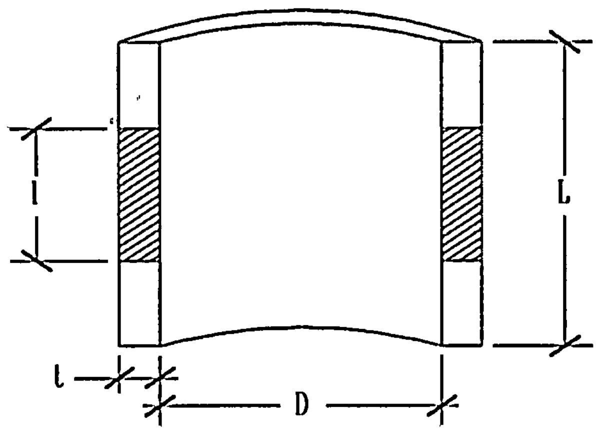

Figure 5-2 Partial Shell Section

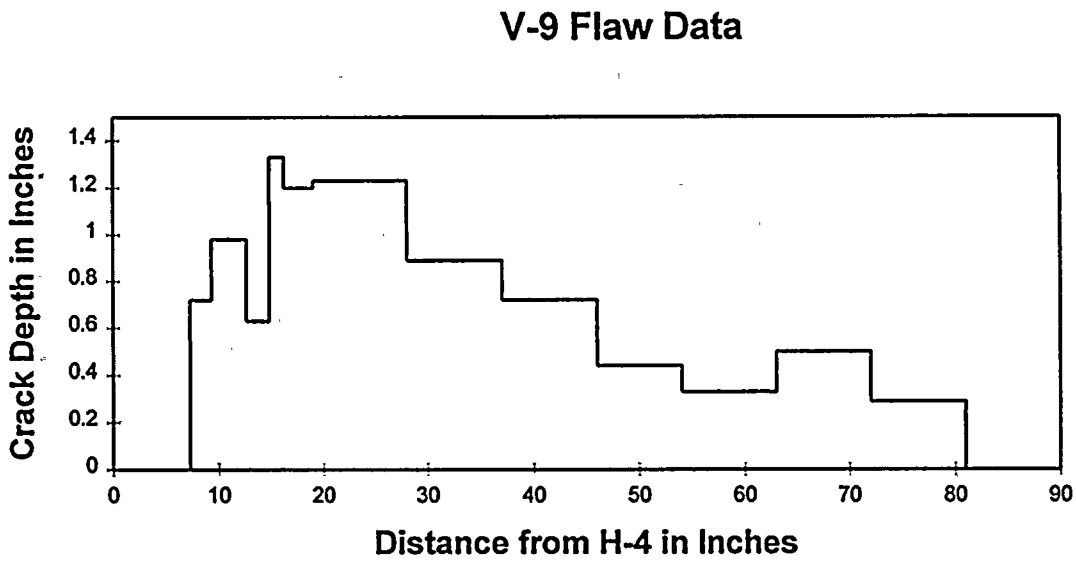

Figure 5-3 V-9 Flaw Data

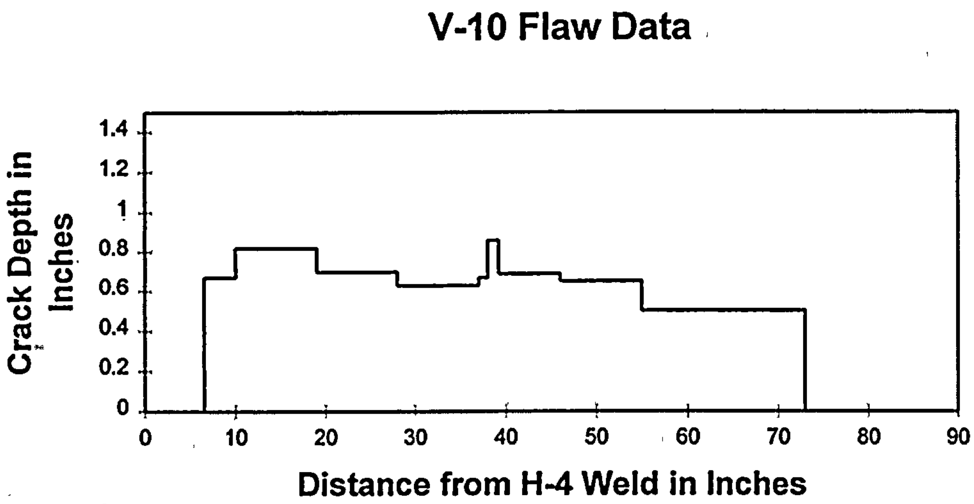

Figure 5-4 V-10 Flaw Data

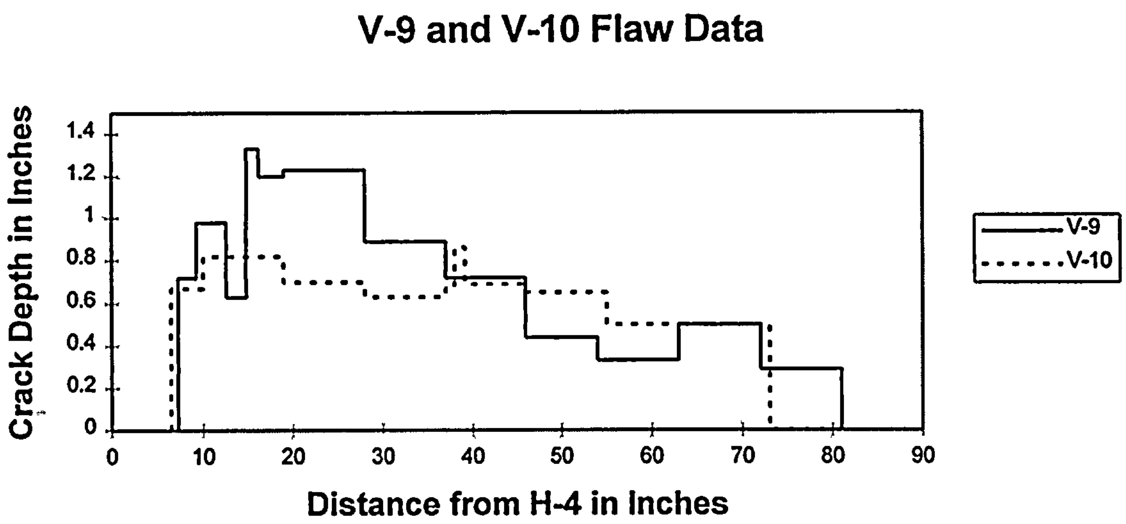

Figure 5-5 Comparison of V-9 and V-10 Flaw Data

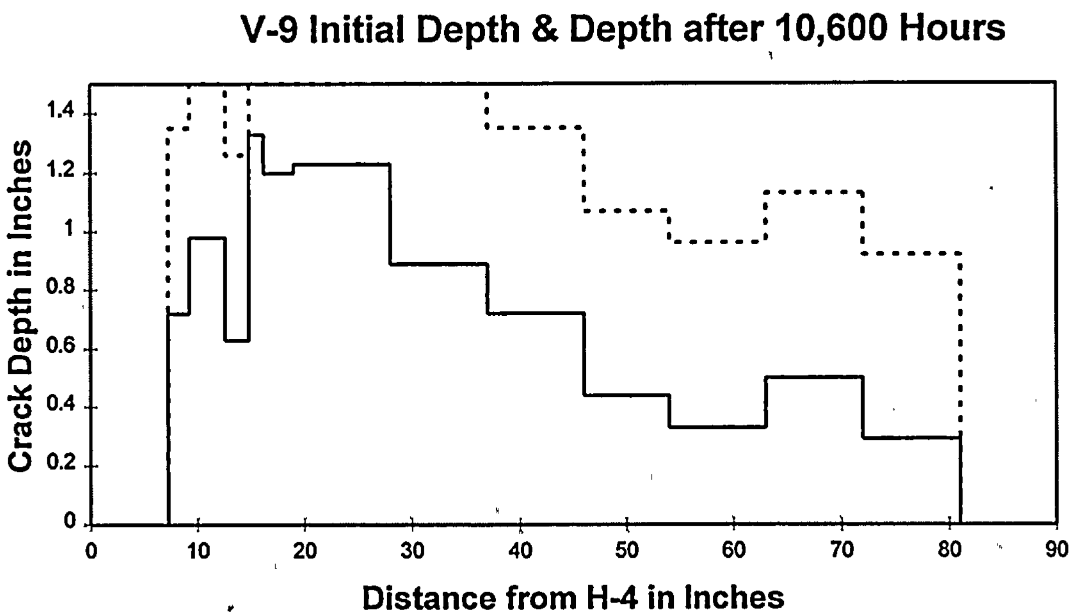

Figure 5-6 V-9 Crack Depth after 10,600 Hours

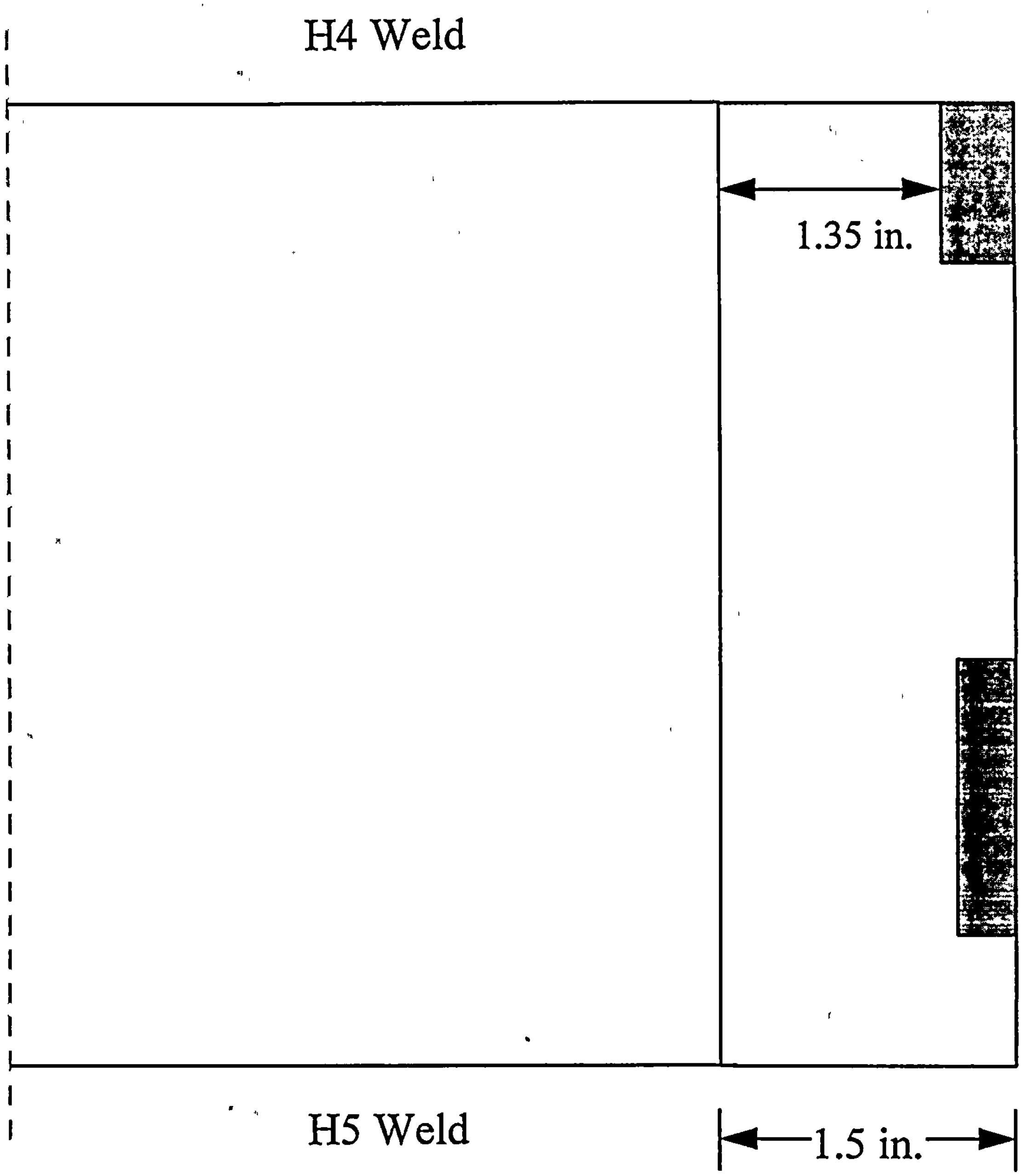

Figure 5-7 Idealized Compound Crack for V-9

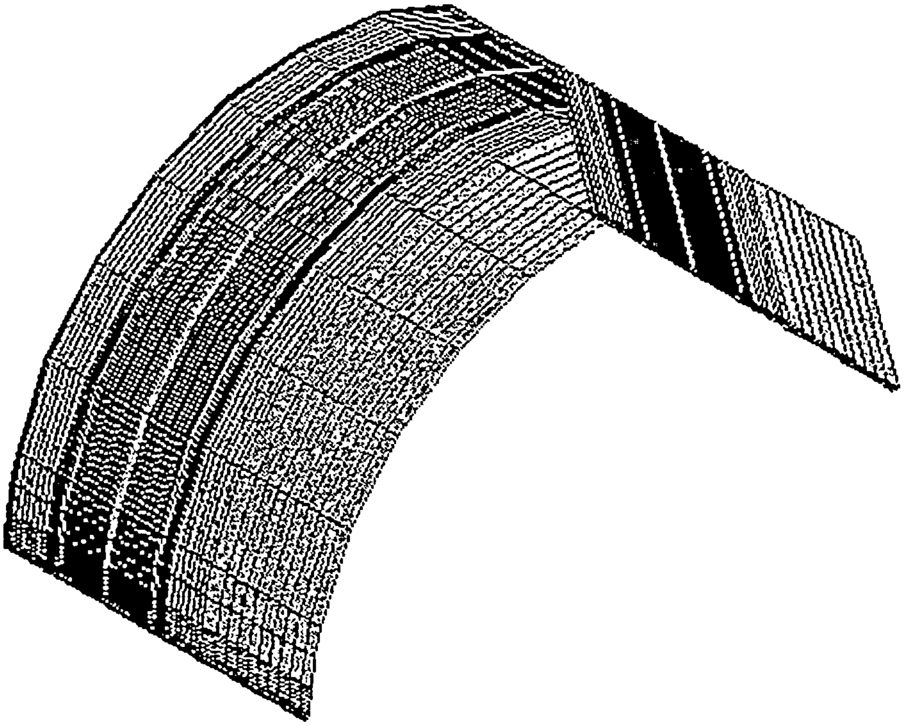

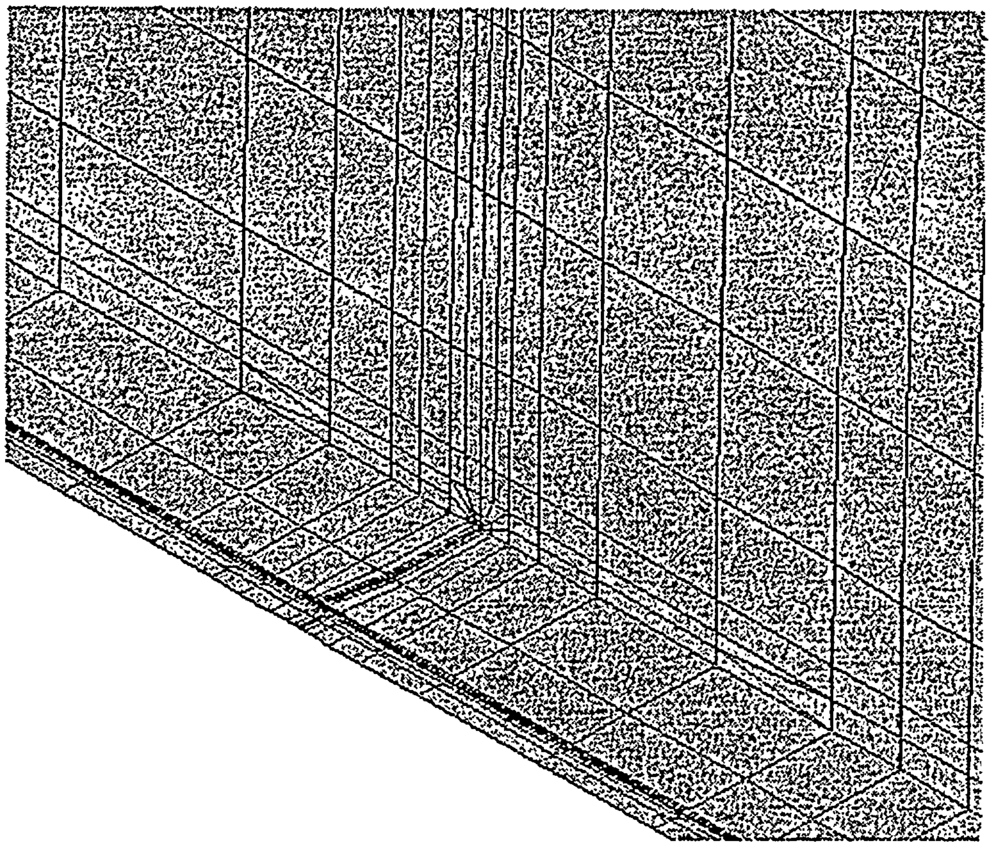

Figure 5-8 Finite Element Model of the Shroud Section

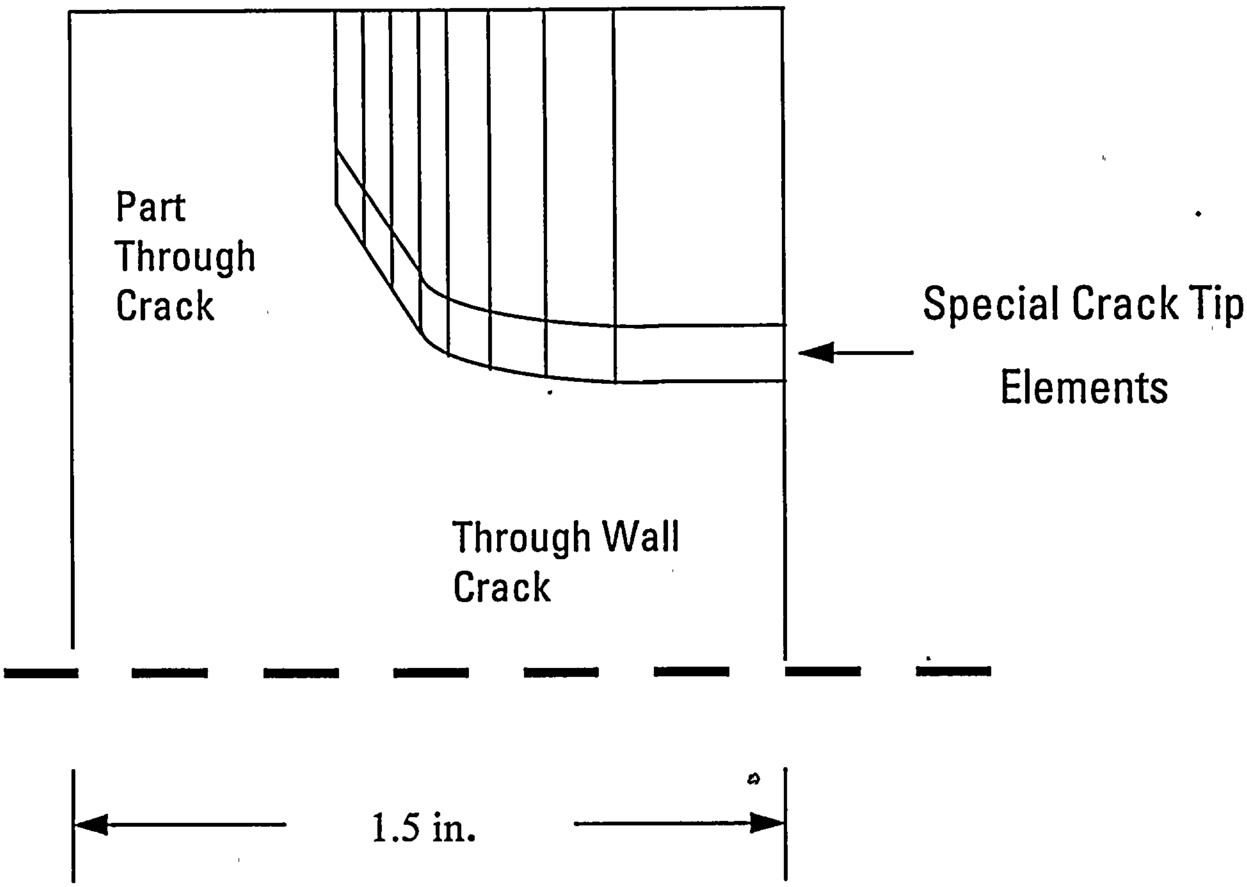

Figure 5-9 Details of the Crack Tip Region Showing the Special Crack Tip Elements

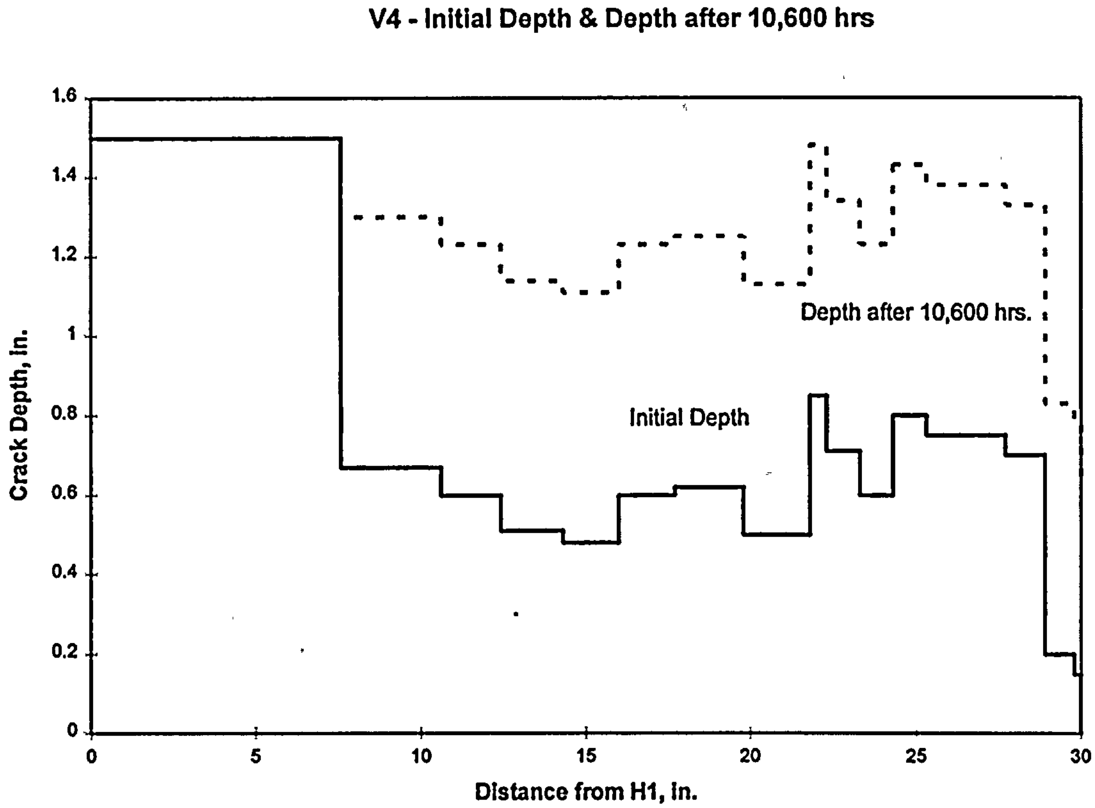

Figure 5-10 V-4 Initial Depth and Depth After 10,600 Hours

Table 5-1
Reactor Internal Pressure Differentials

Event	H-1 to H-2 ΔP	H-3 to H-6a ΔP	Below Core Plate ΔP
Normal and Upset	8.9 psi	8.9 psi	23.6 psi
Faulted	22 psi	22 psi	63.0 psi

Table 5-2
Allowable Flaw Sizes for the Nine Mile Point Unit 1 Shroud Vertical Welds

(1) Weld ID	(2) Weld Length, in	(3) Allowable Through wall crack length, in. LEFM	Limit Load	(4) Minimum required ligament, in.	(5) Min. Ligament including crack growth (two years) and Inspection Uncertainty, in. (Note 1)	(6) Available Equivalent Uncracked Ligament Length, in.
V-3, V-4	31.25	-	29.97	1.28	3.63	7.3 (V-3) Note 2 (V-4)
V-7, V-8	18.50	18.3	17.78	0.72	3.07	9.0 (V-7) 5.6 (V-8)
V-9, V-10	90.12	75.40	86.61	14.72	17.07	Note 2 (V-9) Note 2 (V-10)
V-11, V-12	63.50	58.20	61.03	5.30	9.30 Note 3	31.75 (V-11) 25.75 (V-12)
V-15, V-16	22.13	-	19.53	2.46	4.81	Note 4 (V-15) 5.5 (V-16)

Notes

1. Based on crack growth of 1.6 in. and UT inspection uncertainty of 2 x 0.375 inch at each crack tip for length sizing.
2. Meets requirements based on further evaluation reported in Subsection 5.3.
3. The minimum ligament for EVT inspection is larger to account for greater uncertainty in the visual inspection. The uncertainty factor applied is equal to 2 x 1.2 in.
4. The equivalent length after subtracting crack growth and inspection uncertainty is 2.89 in. which is greater than the required ligament of 2.46 in. and thus acceptable.

6.0 THERMAL HYDRAULICS ASSESSMENT

An evaluation was performed to assess the potential leakage through shroud vertical weld cracks. The evaluation included an assessment of the impact of nominal leakage with an assumed through wall crack (actual indications do not have through wall cracks) on normal operation, transients and plant safety.

This evaluation has primarily focused on vertical welds V-9 and V-10. Leakage from other vertical welds can be bounded by this evaluation because V-9 and V-10 are the longest vertical welds and the calculated crack opening for the postulated through wall flaw is proportional to the weld length.

The results of the evaluation are provided below.

6.1 Leakage Estimate

The potential crack openings at vertical welds (V-9, V-10, etc.) were determined from a structural analysis and are dependent on the pressure drop across the shroud wall. It was conservatively assumed that the cracks are throughwall. The leakage flow and impact evaluation was performed at 100% rated power and 100% rated core flow (bounds core flows down to 85% at rated power) with applicable reactor internal pressure differences (RIPDs) across the shroud wall. The predicted total leakage flow area for the V-9 and V-10 weld cracks is approximately 3 in^2. The loss coefficients for the leakage flow are determined to take into account both form and frictional losses. The predicted leakage flow is summarized in Table 6-1.

Table 6-1
Summary of Leakage Flows at Rated Conditions

	(gpm)	(% of core mass flow)
Vertical weld cracks, V-9 & 10	200	0.11
Horizontal weld repair	1510	0.54

Leakage flow associated with the hardware previously installed to repair the horizontal weld cracks in the shroud (Reference 5) is included in Table 6-1. The leakage flow for the horizontal weld repair takes into account the as built configuration, with leakage at

eight holes in the shroud head flange, eight holes in the cone, and eight circumferential shroud welds (H-1 - H-7). It is conservatively assumed that each of these welds develops a complete circumferential crack that opens to 0.001 inches.

The predicted leakage flow for the vertical weld cracks plus the horizontal weld repair is about 0.65% of core mass flow, which is small compared to the core flow uncertainty.

6.2 Detectability

A safety assessment of the shroud cracks in the NMP1 plant, prior to the shroud repair, is documented in Reference 7. Based on that assessment, shroud cracks may be detectable provided that a power anomaly of two percent of rated power results from the expected leakage. The maximum leakage expected for the shroud condition is less than one percent. Since approximately a three per cent leakage is required to produce a two per cent power effect, it is concluded that the shroud leakage may not be detectable. Furthermore, other secondary leakage indicators, such as recirculation loop temperature and core support plate pressure differential, are also too small to be distinguishable from normal operation measurements.

However, if the vertical weld crack develops further creating a larger leakage flow area, the crack will be detectable. The threshold for detection of the shroud cracking in the horizontal welds is 1/4 inch (Reference 7), horizontal welds have a much longer length than the vertical welds, V-9 and V-10, by a factor of approximately 6. Therefore, a 1/4 inch lift with the horizontal welds is equivalent to 1.5 inch opening for the V-9 and V-10 welds. When more than 1.5 inch average opening is created for the entire length of the weld, the power decrease will be more than 2 %, and the leakage will be detectable.

6.3 Impact on Plant Performance and Plant Safety

The impact of the leakage flow on the steam separation system performance, cavitation protection, core monitoring, abnormal transients, emergency core cooling system (ECCS) performance and fuel cycle length are evaluated as summarized in the following subsections.

6.3.1 Steam Separation System

The leakage flow through holes in the shroud head and weld cracks H-1 and H-2 occurs above the top guide support ring and includes steam flow, which slightly increases the total carryunder in the downcomer by about 0.02 weight (wt) % at rated power. The total leakage flow also has the effect of slightly decreasing the flow per separator and slightly increasing the separator inlet quality. The separator performance is based on the applicable separator test data over the operating water level range. The combined effective carryunder from the separators and the shroud leakage remains within the design requirement (0.25 wt %). The carryover from the separators remains within the design limit so that moisture from the dryer meets the plant performance requirement of less than 0.1 wt %.

6.3.2 Cavitation Protection

The increased total carryunder due to leakage will decrease the subcooling of the flow in the downcomer slightly. This in turn reduces the margin to cavitation slightly. However, there is no impact compared with the design margin because the total effective carryunder remains within the design requirement.

6.3.3 Core Monitoring

The leakage results in an overprediction of core flow by about 0.7% of core flow. This overprediction is small compared to the core flow measurement uncertainty of 5% for non-jet pump plants (Reference 8) used in the MCPR Safety Limit evaluations. Additionally, the decrease in core flow resulting from the overprediction results in only about 0.2% decrease in calculated MCPR. Therefore, it is concluded that the impact is not significant.

6.3.4 Anticipated Abnormal Transients

The code used to evaluate performance under anticipated abnormal transients and calculate fuel thermal margin includes carryunder as one of the inputs. The effect of the increased carryunder due to shroud repair or postulated vertical throughwall cracks results in greater compressibility of the downcomer region and, hence, a reduced

maximum vessel pressure. Since this is a favorable effect, the thermal limits are not impacted.

6.3.5 Emergency Core Cooling System During LOCA

The Design Basis accident is the recirculation discharge line break LOCA for NMP1 plant which relies solely on Core Spray for mitigation of the LOCA events and the subsequent rewetting of the fuel rods (Reference 9). The effect of the vertical weld cracking on the peak cladding temperature (PCT) during LOCA is determined by whether the core spray flow to the upper plenum region is affected or not. The leakage through the shroud repair holes or vertical or horizontal shroud cracks does not change the core spray flow or the cooling to the fuel rods or fuel channel. Therefore, the LOCA analysis results presented in Reference 9, including PCT and metal water reaction, are unchanged by the shroud leakage, and are applicable.

6.3.6 Fuel Cycle Length

The combined impact of the reduced core inlet subcooling and the reduced core flow due to the leakage results in a minor effect (~2 days) on fuel cycle length and is considered acceptable.

6.4 Conclusion

The impact of the leakage flows through potential vertical weld cracks and the horizontal shroud repair installation have been evaluated. The results show that at rated power and core flow the predicted leakage is sufficiently small so that the steam separation system performance, cavitation protection, core monitoring, fuel thermal margin and fuel cycle length remain adequate. Also, no impact on LOCA analysis has been found and the existing LOCA analysis is applicable.

Cracking in the shroud vertical welds V-9 and V-10 may not be detectable during normal operation because the magnitude of the estimated leakage from the postulated through wall cracking is very small. If the crack opens more than 1.5 inches for the V-9 or V-10 weld, the crack will be detectable.

7.0 OVERALL SAFETY CONCLUSION

Extensive examinations were performed to fully characterize all of the shroud vertical welds. A detailed evaluation was performed for all of the vertical welds to determine the structural significance of the indications. Several conservative assumptions were made in the analysis:

- No credit was taken for horizontal welds; it is assumed that each section of the shroud is a free standing cylinder. Thus the presence of horizontal weld cracking has no impact on the vertical weld crack assessment,

- A bounding crack growth rate of 5×10^{-5} inches per hour has been assumed. Field data and predictive models show that this is bounding even with irradiation effects. Furthermore, because of the excellent water chemistry at NMP1 (reactor water conductivity <0.1 μS/cm), the actual crack growth rates are expected to be much lower,

- All uninspected regions are postulated to be cracked throughwall, and allowance is made for crack sizing uncertainty for detected flaws.

- The results of the fracture mechanics analysis demonstrate that continued operation can be justified for at least 10,600 hours (approximately 16 months). The results of the thermal hydraulic evaluation showed that even with postulated through wall cracking of the vertical welds the resulting leakage has no safety impact. Furthermore, since the vertical weld cracks are within the allowable sizes, they have no impact on the effectiveness of the shroud repair which structurally replaces the horizontal welds.

Based on the evaluation presented, continued operation can be justified for 10,600 hours (approximately 16 months).and all of the required safety margins will be maintained.

8. REFERENCES

1. BWRVIP Document, EPRI TR-105747, "Guidelines for Reinspection of Core Shrouds (BWRVIP–07)", February 1996.
2. BWRVIP Document, EPRI TR-105696, "Reactor Pressure Vessel and Internals Examination Guidelines (BWRVIP-03)", October, 1995.
3. BWRVIP Document, EPRI TR- 105873, "Evaluation of Crack Growth BWR Stainless Steel RPV Internals, (BWRVIP-14)", March 1996.
4. Gott, Karen, "Using Materials Research Results in New Regulations - The Swedish Approach," Proceedings of Seventh International Symposium on Environmental Degradation of Materials in Nuclear Power Systems - Water Reactors, Volume 1 (pp. 639-649), August 1995.
5. GE Document GENE-B13-01739-04, "Nine Mile Point Unit 1 Shroud Repair Hardware Stress Analysis", January 1995.
6. H. Tad, P.C. Paris and G.R. Irwin, "The Stress Analysis of Cracks Handbook", Second Edition (1985).
7. GE Document GENE-523-A093-0995, " Nine Mile Point 1 and Oyster Creek Shroud Safety Assessment", December 1996.
8. "General Electric Fuel Bundle Designs", Volume 1, General Electric Company, June 1996 (NEDE-31152P)
9. D.K. Rao, et al, "Nine Mile Point Unit 1 Loss-of-Coolant Accident Analysis With Two Spargers Available", General Electric Company, September 1993 (NEDC-31446P Supplement 4).

Appendix A

Effect of Tie Rod Loads on Vertical Weld Stresses

Effect of Tie Rod Loads on V-9 and V-10 Vertical Weld Stresses

A-1. Objective

The NMP1 shroud modification system consists of four sets of tie rod assemblies between the shroud support cone and the shroud head support ring. The tie rods are mechanically and thermally pre-loaded with sufficient clamping force to prevent separation of shroud sections at postulated circumferential weld cracks under normal operating pressures. The analyses described in this note demonstrate that this preload would produce insignificant loads across the V-9 and V-10 vertical welds in the shroud (Figure 1).

A-2. Analyses

Finite element analyses were performed to calculate the stresses from the operating load in each of the tie rods assuming all four tie rods maintain the design preload.

A-2.1 Analysis Model

Shroud stresses from the tie rod loads were calculated in finite element analyses using the ANSYS (version 4.4A) computer code. The 180 ° analysis model shown in Figure 2 was composed of solid elements including rotational degrees of freedom (ANSYS element STIF4). The solid elements were used to model the shroud head support ring, top guide support ring, core plate support ring, and the stainless steel transition ring. The shell elements were used to model the cylindrical sections of the shroud and shroud support cone. Beam elements were used to model the tie rods.

The use of the shell elements in the analysis model (instead of an entire solid elements model) was dictated by the need to limit the model size. Except for the top guide support ring, the interfaces between the shell elements and solid elements were modeled by extending the shell elements to cover the surfaces of the solid element rings in order to assure transfer of bending deformations. The surface shell elements in these cases had the

same thickness as the shroud thickness and the widths of the underlying solid element rings were decreased by corresponding amounts. The full width of the top guide support ring was modeled with solid elements and the shroud sections above and below the ring were assumed to contact the ring at the shroud ID and shroud OD, respectively. The tie rod at 90° was modeled with the full tie rod section properties while the rods at 0° and 180° were modeled with half-section properties as required by the 180 °shroud model.

A-2.2 Boundary Condition

The shroud was assumed to be supported at the reactor vessel interface with the shroud support cone. Symmetry conditions were applied at 0° and 180°.

The tie rod loads were simulated as thermal loads by appropriate changes in the tie rod temperatures relative to the shroud temperature. The temperature difference was selected to produce the normal operation load in the tie rod at 90° and half of the load at the 0° and 180° in the 180° analysis model.

A-2.3 Analysis Results

The calculated hoop stresses in the entire shroud (for a unit load case with tie rod load equal to 69.5 kips) are shown in Figure 3. The stress variation in the shell follows the typical pattern of bending stresses in shells attached to a stiff-ring. The tie rod loads produce compressive hoop stress in the shell immediately below the top guide support ring. The compressive stress decreases with distance for the top guide support changing into tension which reaches a maximum value and then decreases to a small value along the shroud length. The maximum tensile stress across V-9 and V-10 is negligibly small.

A-3. Summary and Conclusions

The operational preload in the tie rods will produce a negligibly small tensile hoop stress across the V-9 and V-10 vertical welds. The stresses are insignificant compared to the stresses required for crack initiation and growth of existing flaws.

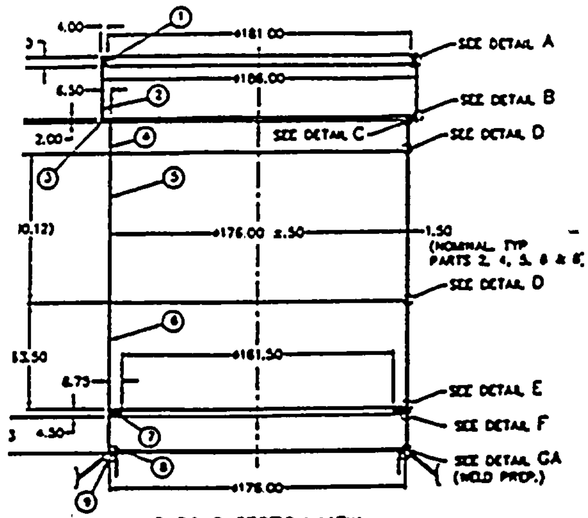

SHROUD SECTION VIEW

PART NUMBER	PART NAME	QUANTITY	MATERIAL TYPE	HEAT NUMBER	CARBON CONTENT - %	COMMENTS ON MATERIAL / PROCESS
1	UPPER RING	2 PIECES	A240 TYPE 304	65444-1	064	PLATE
2	UPPER CYLINDER	2 PIECES	A240 TYPE 304	65235-1A 65235-1B	.042 .042	
3	CENTRAL RING	2 PIECES	A240 TYPE 304	65294-1	056	
4	CENTRAL UPPER CYLINDER	2 PIECES	A240 TYPE 304	65235-1	.042	
5	CENTRAL MID CYLINDER	2 PIECES	A240 TYPE 304	65291-1A 840784-2 65290-1 65235-1	032 033 047 042	
6	CENTRAL LOWER CYLINDER	2 PIECES	A240 TYPE 304	65290-1A 840784-2B 840784-2A 65291-1	047 033 033 .032	
7	LOWER RING	2 PIECES	A240 TYPE 304	65444-1	.064	
8	LOWER CYLINDER	2 PIECES	A240 TYPE 304	65291-1 840784-2A 840784-2B 65290-1A	032 033 033 047	
9	SHROUD SUPPORT RING	1 PIECE	ASME SA-336 F8	C-23/243352	NOT KNOWN	FORGING

NINE MILE POINT 1 SHROUD DATA

NOTES:
1. HEAT NUMBER DATA SHOWN MAY BE APPLICABLE FOR NINE MILE POINT 1 AND/OR OYSTER CREEK.

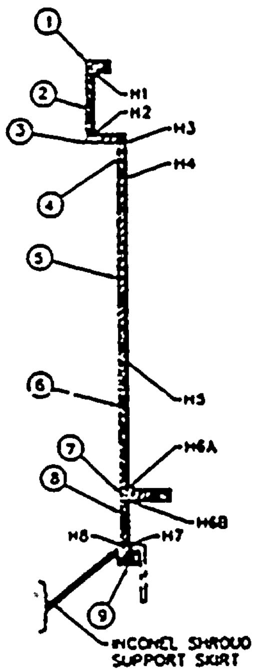

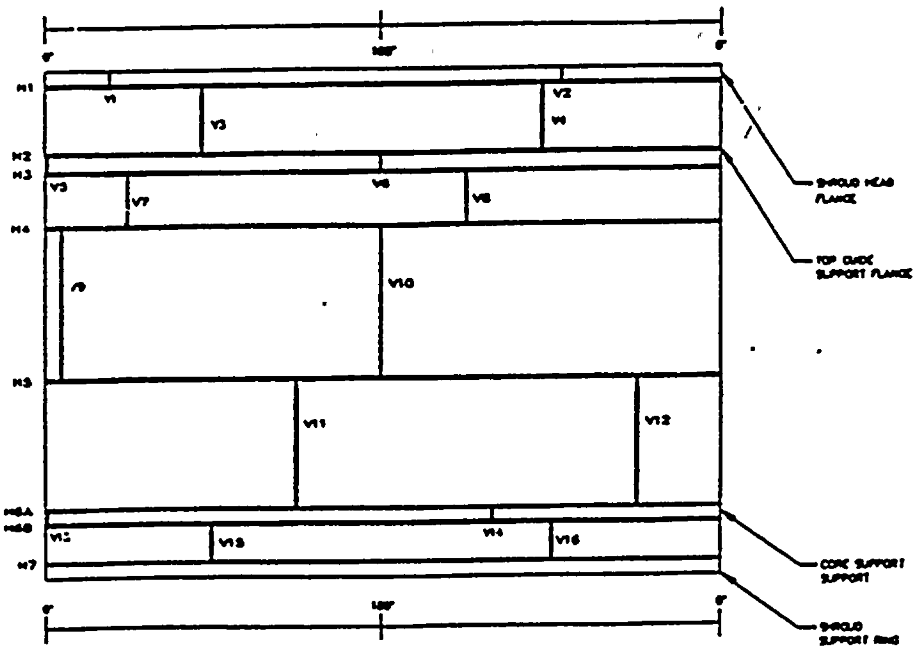

SHROUD SURFACE DEVELOPMENT

Figure 1.1: Shroud Weld Locations

1

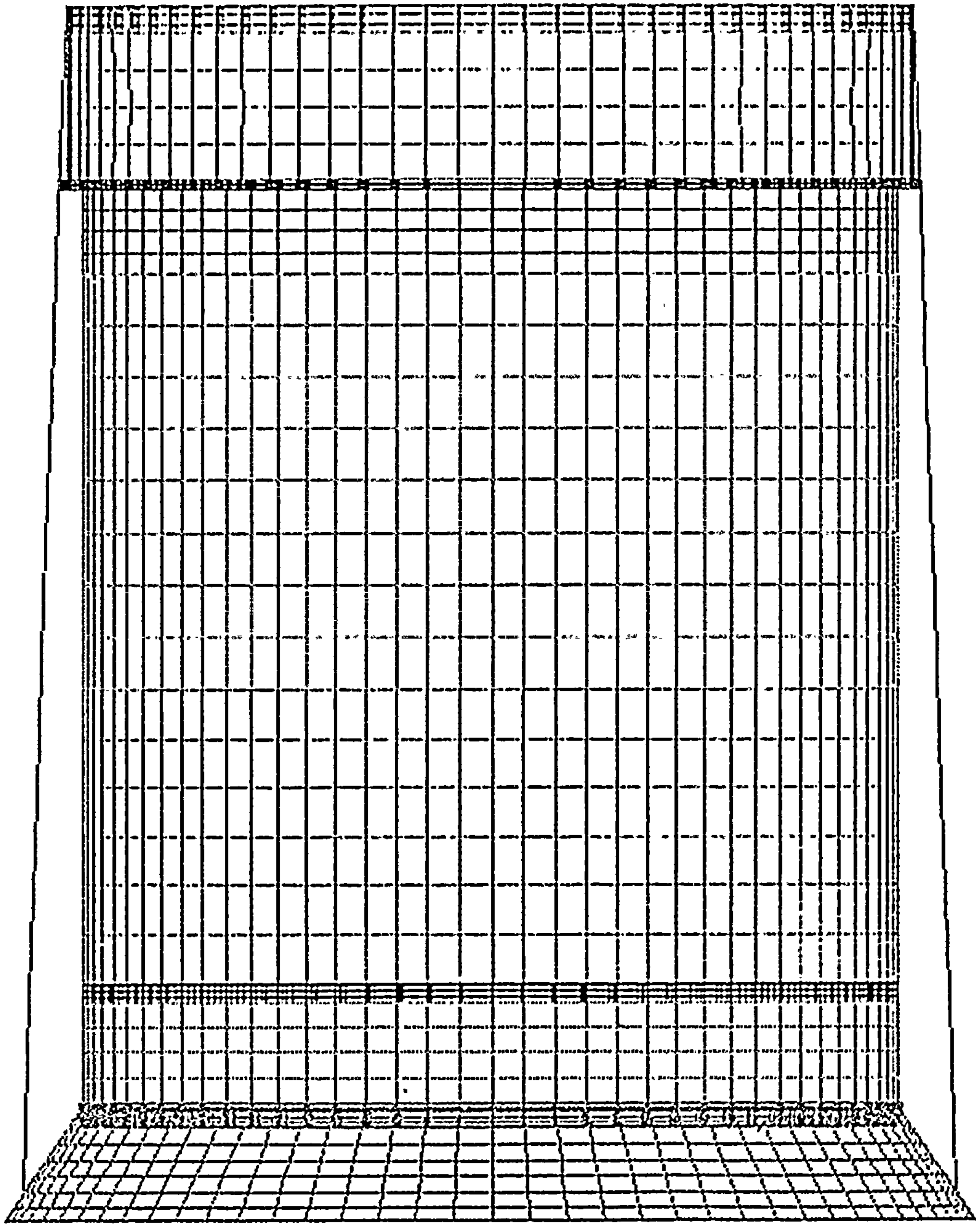

ANSYS 4.4A1
MAR 31 1997
10:46:46
PREP7 ELEMENTS
TYPE NUM

YV =-1
*DIST=144.627
*YF =53.25
*ZF =258.521

180-degrees model

shroud : four tie-rods

Figure 2. Analysis Model
(Four tie-rods)

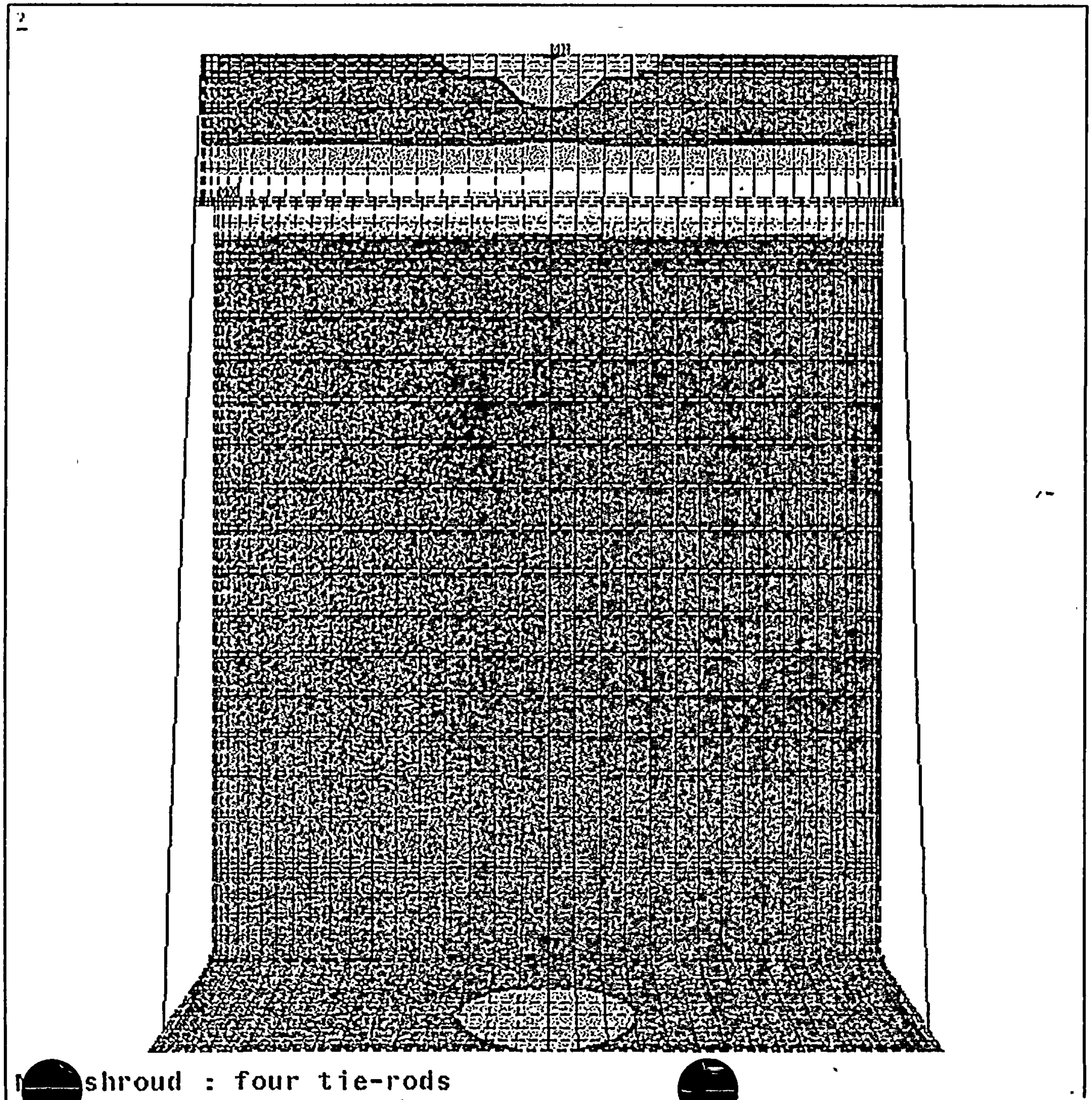

Figure 3. Hoop Stresses

(Four tie-rods)

Appendix B

Crack Growth Rate Based on the GE Theoretical Model

Crack Growth Rate Based on the GE Theoretical Model

The crack growth rate is based on the GE theoretical model and is derived from an estimated average stress intensity factor through the thickness of the shroud.

The Nine Mile 1 shroud cylinder was fabricated from roll formed Type 304 stainless steel plate. Therefore, the weld heat-affected-zone (HAZ) is likely sensitized. The shroud is also subjected to neutron fluence during the reactor operation which further increases the effective degree of sensitization. The other side effect of neutron fluence induced irradiation is the relaxation of weld residual stresses. The theoretical model developed by GE quantitatively considers the degree of sensitization, the stress state and the water environment parameters, in predicting a stress corrosion cracking (SCC) growth rate. The crack growth rate predicted by this model is described next.

Figure B-1 schematically shows the GE theoretical (also called, slip-dissolution film-rupture) model for crack propagation. The crack propagation rate, V_t is defined as a function of two constants (A and n) and the crack tip strain rate. The values of the constants are dependent on the material condition (Electrochemical Potentiokinematic Reactivation or EPR value) and the environment (water conductivity and electro-chemical corrosion potential or ECP) conditions. Constants A and n are related as follows:

$$A = 7.8\mathrm{x}10^{-3}\, n^{3.6} \qquad \text{(B-1)}$$

The crack tip strain rate is formulated in terms of stress, loading frequency, etc. and is obtained as follows:

$$d\varepsilon/dt_{ct} = CK^4 \qquad \text{(B-2)}$$

Where K is the stress intensity factor, a fracture mechanics parameter. When a radiation field, such as the case for the shroud, is present, there is additional interaction between the gamma field and the fundamental parameters which affect intergranular stress corrosion cracking (IGSCC) of Type 304 stainless steel (see Figures B-2 and B-3).

The increase in material sensitization (i.e., EPR) and the changes in the value of constant C as a function of neutron fluence (>1 MeV) is given as the following:

(B-3)

where, EPR is in units of C/cm^2, fluence is in units of n/cm^2 and the calculated value of EPR has an upper limit of .

The constant C is defined as the following:

The units of K to be used with the above expressions is $MPa\sqrt{m}$.

The parameters needed for the crack growth calculation by the GE model are: stress state and stress intensity factor K, effective EPR, water conductivity, and ECP.

The stress state relevant to IGSCC growth rate is the steady state stress which consists of weld residual stress and the steady applied stress. Figure B-4 shows observed through-wall weld residual stress distribution for large diameter pipes. This distribution is expected to be representative for the shroud welds also. The maximum stress at the surface was nominally assumed as 35 ksi. The steady applied stress on the shroud is due to core differential pressure and its magnitude is small compared to the weld residual stress magnitude. Figure B-5 shows the assumed total stress profile used in the evaluation. This stress distribution applies for groove welds similar to those used in joining the vertical seams in the shroud. Figure B-6 shows the calculated values of stress intensity factor (K) assuming a long axial crack. It is seen that the calculated value of K reaches a maximum of approximately 25 $ksi\sqrt{in}$. The average value of K was estimated as 20 $ksi\sqrt{in}$ and was used in the crack growth rate calculations.

The weld residual stress magnitude is expected to decrease as a result of relaxation produced by irradiation-induced creep. Figure B-7 shows the stress relaxation behavior of Type 304 stainless steel due to irradiation at 550° F. Since most of the steady stress in the shroud comes from the weld residual stress, it was assumed that the K values shown in Figure B-6 decrease in the same proportion as indicated by the stress relaxation behavior of Figure B-7.

The second parameter needed in the evaluation is the EPR. In the model, the initial EPR value is assumed as for the weld sensitized condition. Using Equation (B-3), the predicted increase in EPR value as a function of fluence is shown in Figure B-8.

The third parameter used in the GE predictive model is the water conductivity. A water conductivity of 0.1 μS/cm was used in this calculation which represents the current conductivity of most plants. To demonstrate that the GE model conservatively reflects the effect of conductivity, Figure B-10 shows a comparison of the GE model predictions with the measured crack growth rates in the crack advance verification system (CAVS) units installed at several BWRs. The comparison with CAVS data in Figure B-10 also demonstrates the conservative nature of crack growth predictions by the GE model.

The last parameter needed in the GE prediction model is the ECP. Figure B-11 shows the measured values of ECP at two locations in the core. The ECP values at zero H_2 injection in Figure B-11 was used in this calculation. It is seen that the ECP values at zero H_2 injection rate range from 150 mV to 225 mV. Therefore, a value of was used in the calculation.

Based on the preceding, the crack growth rate calculations were conducted as a function of fluence assuming the following values of parameters:

Initial K	= 20 ksi$\sqrt{}$in
EPR_0	=
Cond.	= 0.1 μS/cm^2
ECP	= 200 mV

Figure B-12 shows the predicted crack growth rate as a function of fluence. It is seen that the predicted crack growth rate initially increases with the fluence value but decreases later as a result of significant reduction in the K value due to irradiation induced stress relaxation. The crack growth rate peaks at 4.5x10^{-5} in/hr at a fluence of 1x10^{20} n/cm^2. Thus, a bounding value of 5x10^{-5} in/hr can be conservatively used for the radial direction growth of the existing indication at the shroud welds.

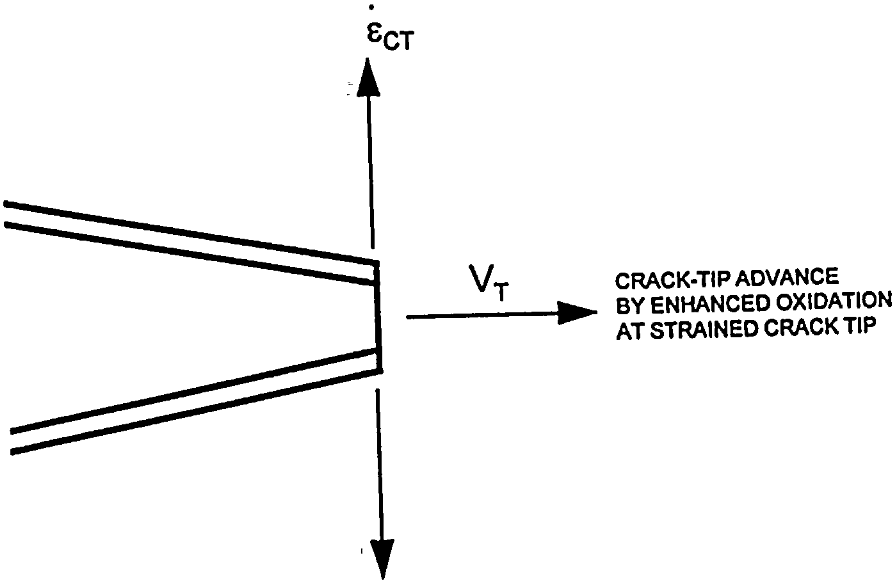

$$V_T = A\,\dot{\varepsilon}_{CT}^{\,n}$$

WHERE:

V_T = CRACK PROPAGATION RATE

A, n = CONSTANTS, DEPENDENT ON MATERIAL AND ENVIRONMENTAL CONDITIONS

$\dot{\varepsilon}_{CT}$ = CRACK-TIP STRAIN RATE, FORMULATED IN TERMS OF STRESS, LOADING FREQUENCY, ETC.

Figure B-1 GE PLEDGE Slip Dissolution-Film Rupture Model of Crack Propagation

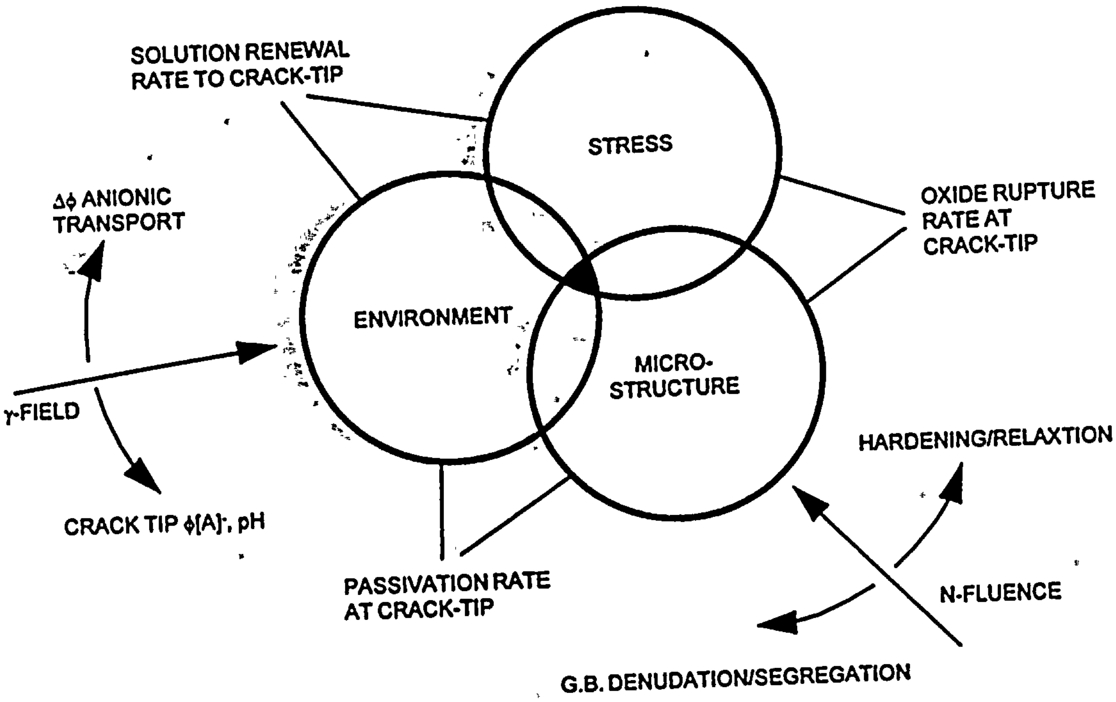

Figure B-2 Effects of Fast Fluence, Flux & Gamma Field on Parameters Affecting IGSCC of Type 304 Stainless Steel

$$V_T = A\dot{\varepsilon}_{CT}^{n}$$

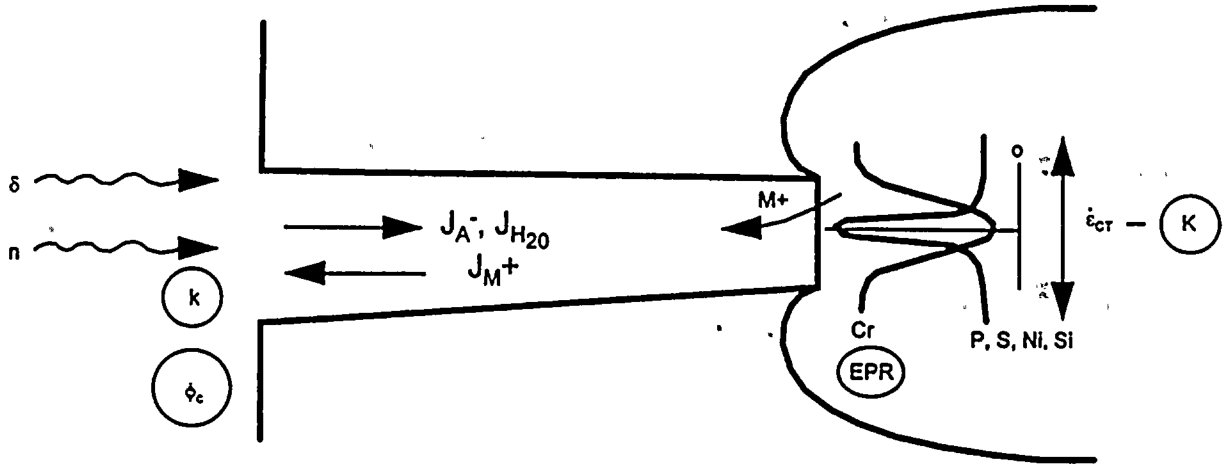

$$V_T = 7.8 \times 10^{-3} n^{3.6} \left[6 \times 10^{-14} K^4\right]^n$$

$$n = \left\{\frac{e^{f(k)}}{e^{f(k)} + e^{f(\phi)c}}\right\}^{f(EPR)}$$

Figure B-3 Parameters of Fundamental Importance to Slip-Dissolution Mechanics of IGSCC in Sensitized Austenitic Stainless Steel

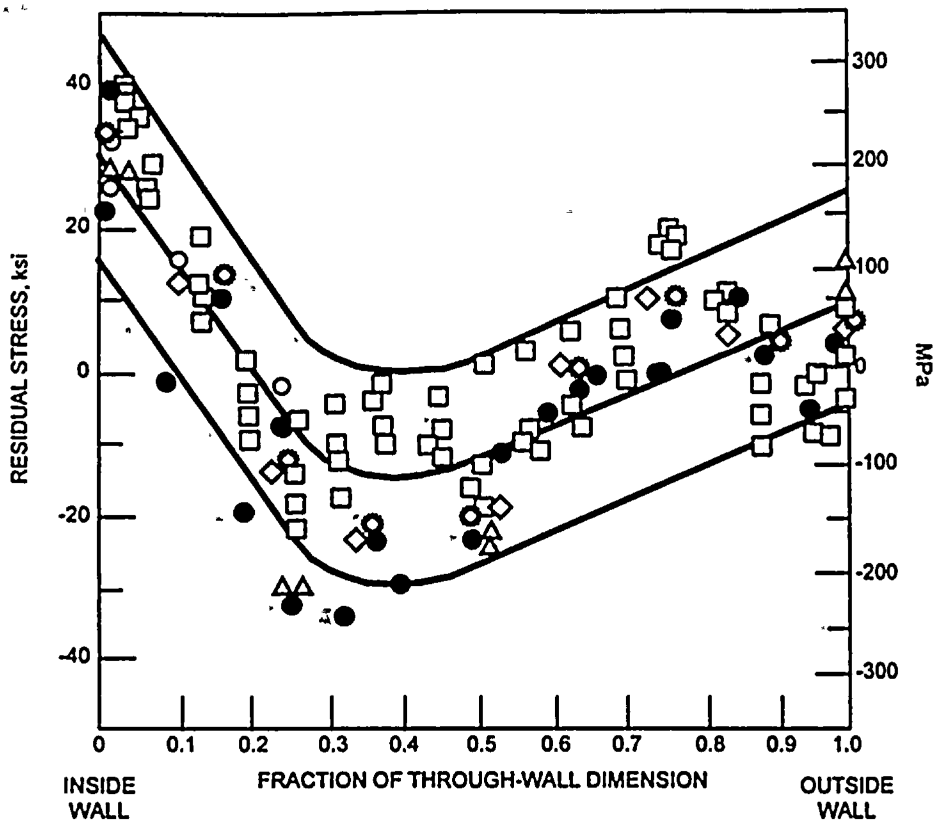

Figure B-4 Throughwall Longitudinal Residual Stress Data Adjacent to Welds in 12 to 28-inch Diameter Stainless Steel Piping

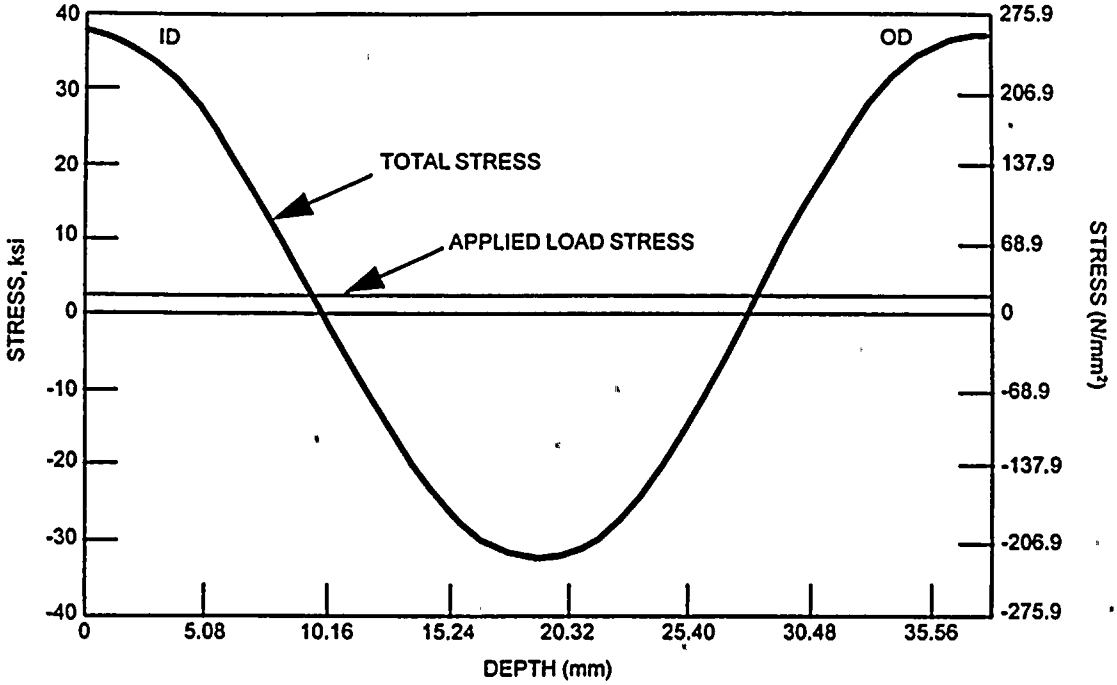

Figure B-5 Shroud Total Throughwall Stress Profile

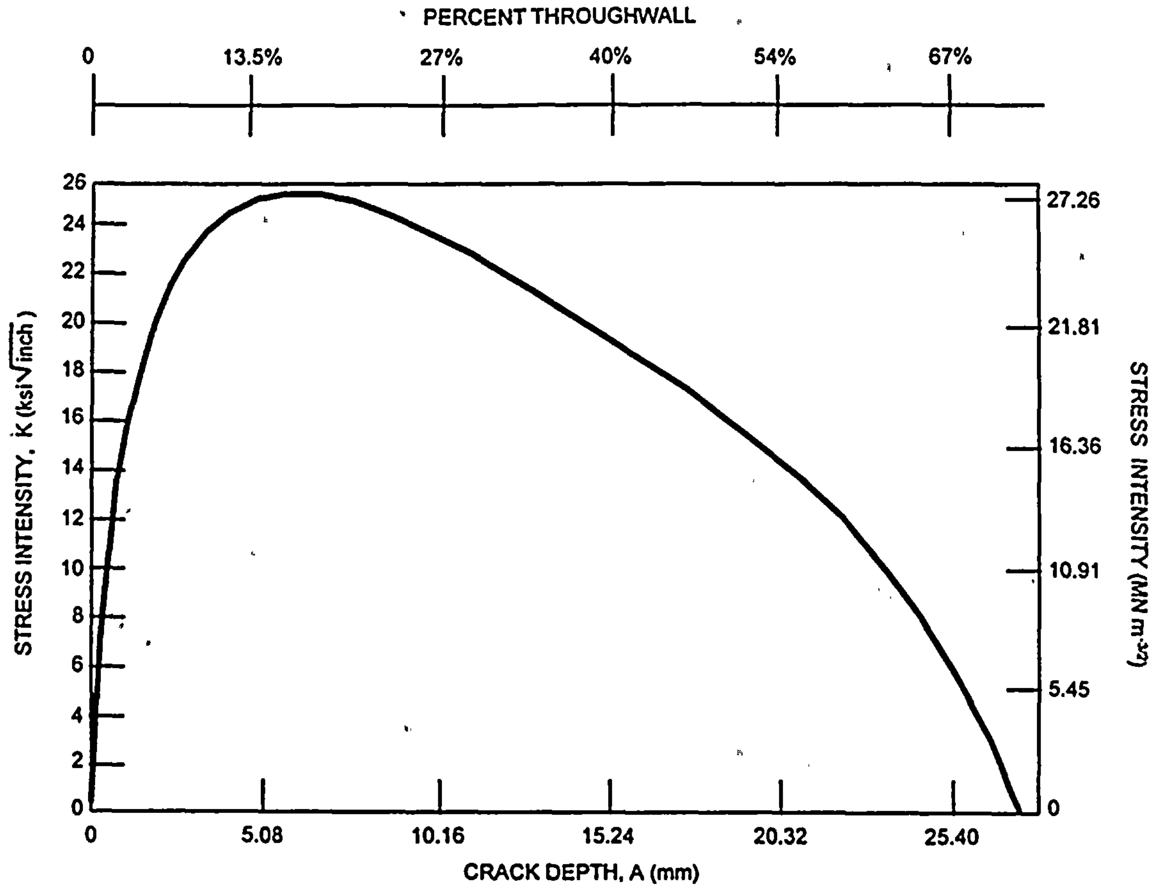

Figure B-6 Shroud Throughwall Stress Intensity Factor

Figure B-7 Stress Relaxation Behavior of Type 304 Stainless Steel Due to Irradiation at 288° C

Figure B-8 EPR Versus Neutron Fluence

Figure B-9 GENE PLEDGE Model Prediction for a BWR 4 Sensitized Type 304 Crack Growth Rate

Figure B-10 Effect of Conductivity on Sensitized Type 304 Crack Growth Rate

Figure B-11 In-Core Bypass ECP Versus Feedwater Hydrogen for a BWR-4

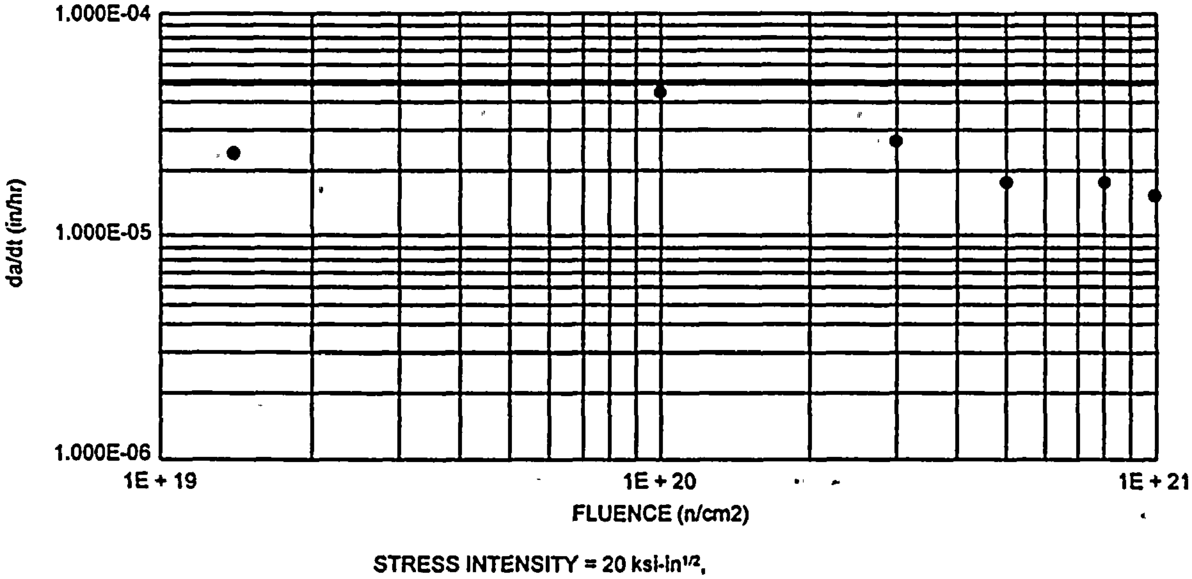

Figure B-12 Growth Rate Versus Fluence

Appendix C
Shroud Inspection Summary

The following is a weld by weld summary detailing the scope of inspections and results of the shroud examinations performed to date.

Weld V-3

Performed ultrasonic examination of approximately 15 inches of each side of the weld from the shroud OD surface. Approximately 1.5" of flaw was detected on the ID surface and 0.8" of flaw on the OD surface.

Weld V-4

Performed ultrasonic examination of approximately 11" of the left HAZ and 22" of the right HAZ. ID flaws were detected over the entire examined length of the left HAZ and 1.5" of flaw was detected on the ID of the right HAZ.

Weld V-7

Performed ultrasonic examination of approximately 9" of the left HAZ and 11" of the right HAZ. No flaws were detected during the examination.

Weld V-8

Performed ultrasonic examination of approximately 5.5" of the left HAZ and 9.5" of the right HAZ. No flaws were detected during the examination.

Weld V-9

Performed ultrasonic examination from the shroud OD surface for approximately the entire length of both the left and right HAZs as well as EVT from both the ID and the OD. Visual cracking was detected over greater than 90% of the right HAZ on the OD and minimal cracking was detected on the ID in both the left an right HAZs. Minor cracking was also detected on the OD in the left HAZ. The cracks detected visually on the shroud ID surface were found to be predominantly transverse to the weld whereas the cracking detected visually on the shroud OD surface was mostly parallel to the weld with components that branched transverse to the weld. Ultrasonic examinations of essentially the entire length of the weld was performed from the shroud OD surface and detected numerous flaws over the length of the left HAZ emanating from the shroud OD surface. Two small flaws on the ID surface were detected in the right HAZ.

Weld V-10

Performed ultrasonic examination from the shroud OD surface for approximately the entire length of both the left and right HAZs as well as EVT from both the ID and the OD. Flaws were detected on greater than 80% of the right HAZ on the OD surface and greater

than 50% of the left HAZ revealed flaws on the OD surface. The EVT examination revealed cracking in the left and right HAZs on the OD surface for most of the length of the weld and on the ID in both the left and right HAZs. The cracks detected visually on the shroud ID surface were found to be predominantly transverse to the weld whereas the cracking detected visually on the shroud OD surface was mostly parallel to the weld with components that branched transverse to the weld.

Weld V-11

EVT examinations were performed on the accessible weld length from both the ID and the OD of both the left and right HAZs. No cracking was detected during the examination.

Weld V-12

EVT examinations were performed on the accessible weld length from both the ID and the OD of both the left and right HAZs. One 6" crack was detected on the length OD surface in the right HAZ. No other cracking was detected.

Weld V-15

Ultrasonic examination was performed from the shroud OD surface on approximately 11 inches of both the left and right HAZs. One 6" flaw was detected in the left HAZ on the ID surface and several ID flaws totaling 2.2" in total length was detected on the ID in the right HAZ. No flaw detected in either HAZ was greater than 10% through wall.

Weld V-16

Ultrasonic examination was performed from the shroud OD surface of approximately 10.5" of left HAZ. Two flaws were detected on the ID surface. One flaw was 5" in length, 10% through wall. The other ID flaw in the left HAZ was detected from the scan on the right HAZ and was 3" long and 30% through wall. Approximately 22 inches of the right HAZ was examine from the shroud OD surface. One flaw was detected on the ID which measured 4" in length and 21% through wall. An EVT examination of both HAZs from the shroud OD surface revealed one crack in the left HAZ.

Recent Inspection Results for Shroud Horizontal Welds

In addition to the shroud vertical weld inspections, the horizontal welds H-2, H-4, H-5, H-6a, H-6b, and H-7 were also inspected for analytical purposes, to evaluate the overall integrity of the shroud using assumptions of worst case cracking of the vertical welds.

Weld H-2

Ultrasonic examination was performed from the shroud OD surface of approximately 24 inches of the upper HAZ adjacent to weld V-4. Approximately 7 inches of intermittent flaws were detected on the OD surface, with the deepest area having a through wall depth of .22 inches.

Weld H-4

Ultrasonic examination from the shroud OD surface was performed on approximately 60% of the lower HAZ. ID and/or OD flaws were detected intermittently throughout the examination area. Some ID flaws were detected in the upper HAZ. Approximately 32 inches of the upper HAZ was ultrasonically examined. 3 inches of shallow OD flaws were detected in the upper HAZ and one 6 inch long ID flaw was detected with the maximum through wall depth of .23 inches. . An EVT examination of the OD was performed of over 70% of the upper and lower HAZs. Cracks were detected in both the upper and lower HAZs.

Weld H-5

Ultrasonic examination from the shroud OD surface was performed on approximately 30% of the upper and lower HAZs. OD and ID flaws were detected in the upper HAZ only. No flaws were detected in the lower HAZ. EVT of approximately 60% of the shroud OD surface revealed cracks intermittently in both the upper and lower HAZs. Most of the flaws detected visually on the OD surface were oriented perpendicular to the weld. No flaws were detected in the upper HAZ at the intersections of welds V9 or V10.

Weld H-6A

Ultrasonic examination was performed on both the upper and lower HAZs of approximately 30% of the circumference from the shroud OD surface. Flaws were detected on the OD surface of the lower HAZ only. No flaws were detected in the upper HAZ or on the ID of either HAZ.

Weld H-6B

Ultrasonic examination was performed on both the upper and lower HAZs of approximately 30% of the circumference from the shroud OD surface. Flaws were detected on the OD surface of the upper HAZ only. No flaws were detected in the lower HAZ or on the ID of either HAZ.

Weld H-7

Ultrasonic examination was performed for the shroud OD surface on the upper HAZ on approximately 30% of the circumference. No flaws were detected during the examination.

Weld H-8

Ultrasonic examination was performed for the shroud OD surface on the lower HAZ on approximately 30% of the circumference. A flaw which was identified by UT during a prior outage was located as well as one additional flaw in the same area. This flaw was ultrasonically sized to be of lesser through wall depth than in RFO13. A review of the previous data indicates that the previous sizing performed was very conservative. An EVT was performed on approximately 30% of the circumference from the shroud OD surface. Of the five small cracks visually detected during RFO13 only 1 was visible during this inspection. The inspection in the area of the other four was hampered by the placement of a Tie Rod support which prevented a good EVT inspection. Cracks were visually detected in three new locations in the upper HAZ. The largest of these cracks (9"-12") is located predominantly in the ring segment Upper HAZ and runs into the weld toe and back into the ring segment.

Weld H-9

An EVT examination was performed in one area 26 inches long. No indications were noted during the examination.